

Chapter 6

Chemical Vapor Deposition

6.1 Selecting a Molecular Precursor for Chemical Vapor Deposition¹

6.1.1 Introduction

The proven utility of chemical vapor deposition (CVD) in a wide range of electronic materials systems (semiconductors, conductors, and insulators) has driven research efforts to investigate the potential for thin film growth of other materials, including: high temperature superconducting metal oxides, piezoelectric material, etc. Moreover, CVD potentially is well suited for the preparation of thin films on a wide range of substrates, including those of nonplanar geometries. CVD offers the advantages of mild process conditions (i.e., low temperatures), control over microstructure and composition, high deposition rates, and possible large scale processing. As with any CVD process, however, the critical factor in the deposition process has been the selection of precursors with suitable transport properties.

6.1.2 Factors in selecting a CVD precursor molecule

The following properties are among those that must be considered when selecting suitable candidates for a CVD precursor:

1. The precursor should be either a liquid or a solid, with sufficient vapor pressure and mass transport at the desired temperature, preferably below 200 °C. Liquids are preferred over solids, due to the difficulty of maintaining a constant flux of source vapors over a non-equilibrium percolation (solid) process. Such non-bubbling processes are a function of surface area, a non-constant variable with respect both to time and particle size. The upper temperature limit is not dictated by chemical factors; rather, it is a limitation imposed by the stability of the mass flow controllers and pneumatic valves utilized in commercial deposition equipment. It must be stressed that while the achievement of an *optimum* vapor pressure for efficient utilization as an industrially practicable source providing high film growth rates (>10 Torr at 25 °C) is a worthy goal, the usable pressure regimes are those in which evaluation can be carried out on compounds which exhibit vapor pressures exceeding 1 Torr at 100 °C.
2. The precursor must be chemically and thermally stable in the region bordered by the evaporation and transport temperatures, even after prolonged use. Early workers were plagued by irreproducible film growth results caused by premature decomposition of source compounds in the bubbler, in transfer lines, and, basically everywhere *except* on the substrate. Such experiences are to be avoided!
3. By its very nature, CVD demands a decomposable precursor. This generally is accomplished thermally; however, the plasma-enhanced growth regime has seen much improvement. In addition, photolytic processes have tremendous potential. Nevertheless, the precursor must be thermally robust *until deposition conditions are employed*.

¹This content is available online at <<http://cnx.org/content/m27846/1.1/>>.

4. The precursor should be relatively easy to synthesize, ensuring sufficient availability of material for testing and fabrication. It also is important that the synthesis of the compound be reproducible. It should be simple to prepare and purify to a relatively high level of purity. It should be non-toxic and *environmentally friendly* (i.e., as low a toxicity as can be attained, given the fundamental toxicity of particular elements such as mercury, thallium, barium, etc.). It should be routine to reproduce and scale-up the preparation for further developmental studies. It should utilize readily available starting reagents, and proceed by a minimum number of chemical transformations in order to minimize the cost.
5. Due to handling considerations, the source should be oxidatively, hydrolytically, thermally and photochemically stable under normal storage conditions, in addition the precursor should resist oligomerization (in the solid, liquid, or gaseous states). It is worth noting that practitioners of metal organic CVD (MOCVD), especially for 13-15 materials have of necessity become expert in the handling of very toxic, highly air sensitive materials.

Historically, researchers were limited in their choices of precursors to those that were readily known and commercially available. It must be emphasized that *none* of these previously known compounds had been designed specifically to serve as vapor phase transport molecules for the associated element. Thus, the scope was often limited to what was commercially available. However, as new compounds have now been made with the specific goal of providing ideal CVD precursors the choice to academia and industry has increased.

6.1.3 Bibliography

- G. B. Stringfellow, *Organometallic Vapor Phase Epitaxy: Theory and Practice*, Academic Press, New York (1989).

6.2 Determination of Sublimation Enthalpy and Vapor Pressure for Inorganic and Metal-Organic Compounds by Thermogravimetric Analysis²

6.2.1 Introduction

Metal compounds and complexes are invaluable precursors for the chemical vapor deposition (CVD) of metal and non-metal thin films. In general, the precursor compounds are chosen on the basis of their relative volatility and their ability to decompose to the desired material under a suitable temperature regime. Unfortunately, many readily obtainable (commercially available) compounds are not of sufficient volatility to make them suitable for CVD applications. Thus, a *prediction* of the volatility of a metal-organic compounds as a function of its ligand identity and molecular structure would be desirable in order to determine the suitability of such compounds as CVD precursors. Equally important would be a method to determine the vapor pressure of a potential CVD precursor as well as its optimum temperature of sublimation.

It has been observed that for organic compounds it was determined that a rough proportionality exists between a compound's melting point and sublimation enthalpy; however, significant deviation is observed for inorganic compounds.

Enthalpies of sublimation for metal-organic compounds have been previously determined through a variety of methods, most commonly from vapor pressure measurements using complex experimental systems such as Knudsen effusion, temperature drop microcalorimetry and, more recently, differential scanning calorimetry (DSC). However, the measured values are highly dependent on the experimental procedure utilized. For example, the reported sublimation enthalpy of $\text{Al}(\text{acac})_3$ (Figure 6.1a, where $M = \text{Al}$, $n = 3$) varies from 47.3 to 126 kJ/mol.

²This content is available online at <<http://cnx.org/content/m33649/1.2/>>.

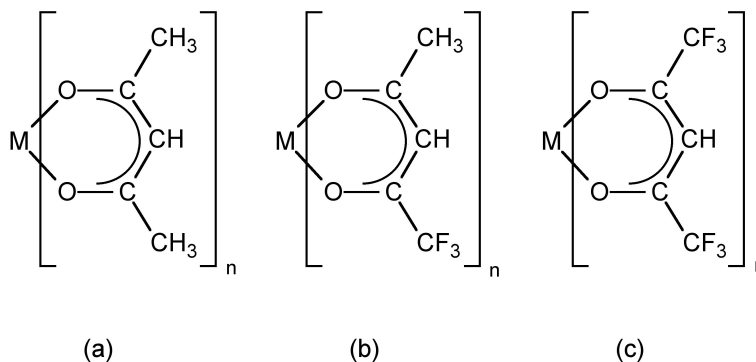


Figure 6.1: Structure of a typical metal β -diketonate complex. (a) acetylacetonate (acac); (b) trifluoroacetylacetonate (tfac), and (c) hexafluoroacetylacetonate (hfac).

Thermogravimetric analysis offers a simple and reproducible method for the determination of the vapor pressure of a potential CVD precursor as well as its enthalpy of sublimation.

6.2.2 Determination of sublimation enthalpy

The enthalpy of sublimation is a quantitative measure of the volatility of a particular solid. This information is useful when considering the feasibility of a particular precursor for CVD applications. An ideal sublimation process involves no compound decomposition and only results in a solid-gas phase change, i.e., (6.1).



Since phase changes are thermodynamic processes following zero-order kinetics, the evaporation rate or rate of mass loss by sublimation (m_{sub}), at a constant temperature (T), is constant at a given temperature, (6.2). Therefore, the m_{sub} values may be directly determined from the linear mass loss of the TGA data in isothermal regions.

$$m_{\text{sub}} = \frac{\Delta[\text{mass}]}{\Delta t} \quad (6.2)$$

The thermogravimetric and differential thermal analysis of the compound under study is performed to determine the temperature of sublimation and thermal events such as melting. Figure 6.2 shows a typical TG/DTA plot for a gallium chalcogenide cubane compound (Figure 6.3).

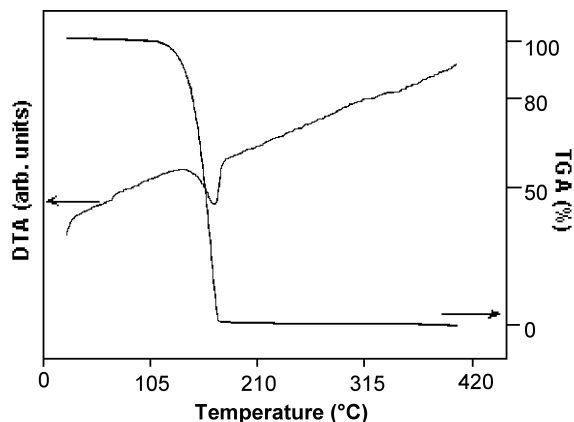


Figure 6.2: A typical thermogravimetric/differential thermal analysis (TG/DTA) analysis of $[(\text{EtMe}_2\text{C})\text{GaSe}]_4$, whose structure is shown in Figure 6.3. Adapted from E. G. Gillan, S. G. Bott, and A. R. Barron, *Chem. Mater.*, 1997, **9**, 3, 796.

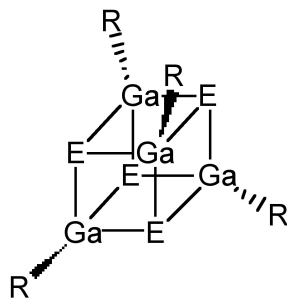


Figure 6.3: Structure of gallium chalcogenide cubane compound, where E = S, Se, and R = CMe_3 , CMe_2Et , CEt_2Me , CEt_3 .

6.2.2.1 Data collection

In a typical experiment 5 - 10 mg of sample is used with a heating rate of ca. 5 °C/min up to under either a 200-300 mL/min inert (N_2 or Ar) gas flow or a dynamic vacuum (ca. 0.2 Torr if using a typical vacuum pump). The argon flow rate was set to 90.0 mL/min and was carefully monitored to ensure a steady flow rate during runs and an identical flow rate from one set of data to the next.

Once the temperature range is defined, the TGA is run with a preprogrammed temperature profile (Figure 6.4). It has been found that sufficient data can be obtained if each isothermal mass loss is monitored over a period (between 7 and 10 minutes is found to be sufficient) before moving to the next temperature plateau. In all cases it is important to confirm that the mass loss at a given temperature is linear. If it is

not, this can be due to either (a) temperature stabilization had not occurred and so longer times should be spent at each isotherm, or (b) decomposition is occurring along with sublimation, and lower temperature ranges must be used. The slope of each mass drop is measured and used to calculate sublimation enthalpies as discussed below.

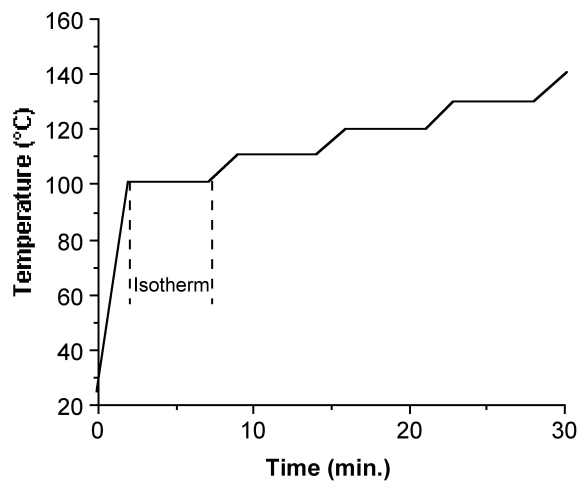


Figure 6.4: A typical temperature profile for determination of isothermal mass loss rate.

As an illustrative example, Figure 6.5 displays the data for the mass loss of $\text{Cr}(\text{acac})_3$ (Figure 6.1a, where $M = \text{Cr}$, $n = 3$) at three isothermal regions under a constant argon flow. Each isothermal data set should exhibit a linear relation. As expected for an endothermal phase change, the linear slope, equal to m_{sub} , increases with increasing temperature.

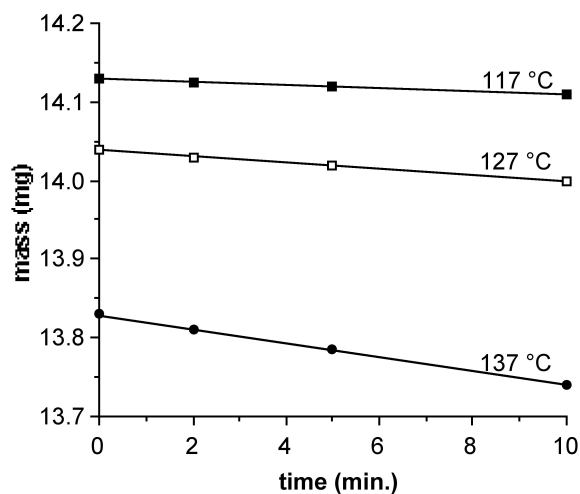


Figure 6.5: Plot of TGA results for $\text{Cr}(\text{acac})_3$ performed at different isothermal regions. Adapted from B. D. Fahlman and A. R. Barron, *Adv. Mater. Optics Electron.*, 2000, **10**, 223.

NOTE: Samples of iron acetylacetonate (Figure 6.1a, where $M = \text{Fe}$, $n = 3$) may be used as a calibration standard through ΔH_{sub} determinations before each day of use. If the measured value of the sublimation enthalpy for $\text{Fe}(\text{acac})_3$ is found to differ from the literature value by more than 5%, the sample is re-analyzed and the flow rates are optimized until an appropriate value is obtained. Only after such a calibration is optimized should other complexes be analyzed. It is important to note that while small amounts ($< 10\%$) of involatile impurities will not interfere with the ΔH_{sub} analysis, competitively volatile impurities will produce higher apparent sublimation rates.

It is important to discuss at this point the various factors that must be controlled in order to obtain meaningful (useful) m_{sub} data from TGA data.

1. The sublimation rate is independent of the amount of material used but may exhibit some dependence on the flow rate of an inert carrier gas, since this will affect the equilibrium concentration of the cubane in the vapor phase. While little variation was observed we decided that for consistency m_{sub} values should be derived from vacuum experiments only.
2. The surface area of the solid in a given experiment should remain approximately constant; otherwise the sublimation rate (i.e., mass/time) at different temperatures cannot be compared, since as the relative surface area of a given crystallite decreases during the experiment the apparent sublimation rate will also decrease. To minimize this problem, data was taken over a small temperature ranges (ca. 30 °C), and overall sublimation was kept low (ca. 25% mass loss representing a surface area change of less than 15%). In experiments where significant surface area changes occurred the values of m_{sub} deviated significantly from linearity on a $\log(m_{\text{sub}})$ versus $1/T$ plot.
3. The compound being analyzed must not decompose to any significant degree, because the mass changes due to decomposition will cause a reduction in the apparent m_{sub} value, producing erroneous results. With a simultaneous TG/DTA system it is possible to observe exothermic events if decomposition occurs, however the clearest indication is shown by the mass loss versus time curves which are no longer linear but exhibit exponential decays characteristic of first or second order decomposition processes.

6.2.2.2 Data analysis

The basis of analyzing isothermal TGA data involves using the Clausius-Clapeyron relation between vapor pressure (p) and temperature (T), (6.3), where ΔH_{sub} is the enthalpy of sublimation and R is the gas constant (8.314 J/K.mol).

$$\frac{d \ln(p)}{dT} = \frac{\Delta H_{\text{sub}}}{RT^2} \quad (6.3)$$

Since m_{sub} data are obtained from TGA data, it is necessary to utilize the Langmuir equation, (6.4), that relates the vapor pressure of a solid with its sublimation rate.

$$p = \left[\frac{2\pi RT}{M_w} \right]^{0.5} m_{\text{sub}} \quad (6.4)$$

After integrating (6.3) in log form, substituting in (6.4), and consolidating the constants, one obtains the useful equality, (6.5).

$$\log(m_{\text{sub}} \sqrt{T}) = \frac{-0.0522(\Delta H_{\text{sub}})}{T} + \left[\frac{0.0522(\Delta H_{\text{sub}})}{T_{\text{sub}}} - \frac{1}{2} \log\left(\frac{1306}{M_w}\right) \right] \quad (6.5)$$

Hence, the linear slope of a $\log(m_{\text{sub}} T^{1/2})$ versus $1/T$ plot yields ΔH_{sub} . An example of a typical plot and the corresponding ΔH_{sub} value is shown in Figure 6.6. In addition, the y intercept of such a plot provides a value for T_{sub} , the calculated sublimation temperature at atmospheric pressure.

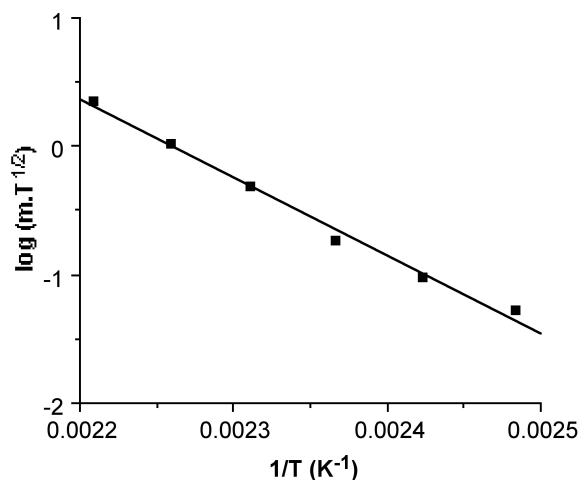


Figure 6.6: Plot of $\log(m_{\text{sub}} T^{1/2})$ versus $1/T$ and the determination of the ΔH_{sub} (112.6 kJ/mol) for $\text{Fe}(\text{acac})_3$ ($R^2 = 0.9989$). Adapted from B. D. Fahlman and A. R. Barron, *Adv. Mater. Optics Electron.*, 2000, **10**, 223.

Table 6.1 lists the typical results using the TGA method for a variety of metal β -diketonates, while Table 6.2 lists similar values obtained for gallium chalcogenide cubane compounds.

Compound	ΔH_{sub} (kJ/mol)	ΔS_{sub} (J/K.mol)	$T_{\text{sub calc.}}$ ($^{\circ}\text{C}$)	Calculated vapor pressure @ 150 $^{\circ}\text{C}$ (Torr)
Al(acac) ₃	93	220	150	3.261
Al(tfac) ₃	74	192	111	9.715
Al(hfac) ₃	52	152	70	29.120
Cr(acac) ₃	91	216	148	3.328
Cr(tfac) ₃	71	186	109	9.910
Cr(hfac) ₃	46	134	69	29.511
Fe(acac) ₃	112	259	161	2.781
Fe(tfac) ₃	96	243	121	8.340
Fe(hfac) ₃	60	169	81	25.021
Co(acac) ₃	138	311	170	1.059
Co(tfac) ₃	119	295	131	3.319
Co(hfac) ₃	73	200	90	9.132

Table 6.1: Selected thermodynamic data for metal β -diketonate compounds determined from thermogravimetric analysis. Data from B. D. Fahlman and A. R. Barron, *Adv. Mater. Optics Electron.*, 2000, **10**, 223.

Compound	ΔH_{sub} (kJ/mol)	ΔS_{sub} (J/K.mol)	$T_{\text{sub calc.}}$ ($^{\circ}\text{C}$)	Calculated vapor pressure @ 150 $^{\circ}\text{C}$ (Torr)
[(Me ₃ C)GaS] ₄	110	300	94	22.75
[(EtMe ₂ C)GaS] ₄	124	330	102	18.89
[(Et ₂ MeC)GaS] ₄	137	339	131	1.173
[(Et ₃ C)GaS] ₄	149	333	175	0.018
[(Me ₃ C)GaSe] ₄	119	305	116	3.668
[(EtMe ₂ C)GaSe] ₄	137	344	124	2.562
[(Et ₂ MeC)GaSe] ₄	147	359	136	0.815
[(Et ₃ C)GaSe] ₄	156	339	189	0.005

Table 6.2: Selected thermodynamic data for gallium chalcogenide cubane compounds determined from thermogravimetric analysis. Data from E. G. Gillan, S. G. Bott, and A. R. Barron, *Chem. Mater.*, 1997, **9**, 3, 796.

A common method used to enhance precursor volatility and corresponding efficacy for CVD applications is to incorporate partially (Figure 6.1b) or fully (Figure 6.1c) fluorinated ligands. As may be seen from Table 6.1 this substitution does results in significant decrease in the ΔH_{sub} , and thus increased volatility. The observed enhancement in volatility may be rationalized either by an increased amount of intermolecular repulsion due to the additional lone pairs or that the reduced polarizability of fluorine (relative to hydrogen) causes fluorinated ligands to have less intermolecular attractive interactions.

6.2.3 Determination of sublimation entropy

The entropy of sublimation is readily calculated from the ΔH_{sub} and the calculated T_{sub} data, (6.6).

$$\Delta S_{\text{sub}} = \frac{\Delta H_{\text{sub}}}{T_{\text{sub}}} \quad (6.6)$$

Table 6.1 and Table 6.2 show typical values for metal β -diketonate compounds and gallium chalcogenide cubane compounds, respectively. The range observed for gallium chalcogenide cubane compounds ($\Delta S_{\text{sub}} = 330 \pm 20 \text{ J/K.mol}$) is slightly larger than values reported for the metal β -diketonates compounds ($\Delta S_{\text{sub}} = 130 - 330 \text{ J/K.mol}$) and organic compounds ($100 - 200 \text{ J/K.mol}$), as would be expected for a transformation giving translational and internal degrees of freedom. For any particular chalcogenide, i.e., $[(R)\text{GaS}]_4$, the lowest ΔS_{sub} are observed for the Me_3C derivatives, and the largest ΔS_{sub} for the Et_2MeC derivatives, see Table 6.2. This is in line with the relative increase in the modes of freedom for the alkyl groups in the absence of crystal packing forces.

6.2.4 Determination of vapor pressure

While the sublimation temperature is an important parameter to determine the suitability of a potential precursor compounds for CVD, it is often preferable to express a compound's volatility in terms of its vapor pressure. However, while it is relatively straightforward to determine the vapor pressure of a liquid or gas, measurements of solids are difficult (e.g., use of the isoteniscopic method) and few laboratories are equipped to perform such experiments. Given that TGA apparatus are increasingly accessible, it would therefore be desirable to have a simple method for vapor pressure determination that can be accomplished on a TGA.

Substitution of (6.2) into (6.4) allows for the calculation of the vapor pressure (p) as a function of temperature (T). For example, Figure 6.7 shows the calculated temperature dependence of the vapor pressure for $[(\text{Me}_3\text{C})\text{GaS}]_4$. The calculated vapor pressures at 150°C for metal β -diketonates compounds and gallium chalcogenide cubane compounds are given in Table 6.1 and Table 6.2.

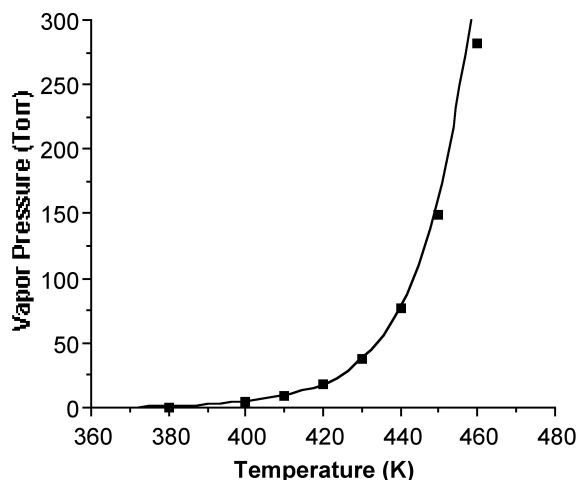


Figure 6.7: A plot of calculated vapor pressure (Torr) against temperature (K) for $[(\text{Me}_3\text{C})\text{GaS}]_4$. Adapted from E. G. Gillan, S. G. Bott, and A. R. Barron, *Chem. Mater.*, 1997, **9**, 3, 796.

The TGA approach to show reasonable agreement with previous measurements. For example, while the value calculated for $\text{Fe}(\text{acac})_3$ (2.78 Torr @ 113 °C) is slightly higher than that measured directly by the isoteniscopic method (0.53 Torr @ 113 °C); however, it should be noted that measurements using the sublimation bulb method obtained values much lower (8×10^{-3} Torr @ 113 °C). The TGA method offers a suitable alternative to conventional (direct) measurements of vapor pressure.

6.2.5 Bibliography

- P. W. Atkins, *Physical Chemistry*, 5th ed., W. H. Freeman, New York (1994).
- G. Beech and R. M. Lintonbon, *Thermochim. Acta*, 1971, **3**, 97.
- B. D. Fahlman and A. R. Barron, *Adv. Mater. Optics Electron.*, 2000, **10**, 223.
- E. G. Gillan, S. G. Bott, and A. R. Barron, *Chem. Mater.*, 1997, **9**, 3, 796.
- J. O. Hill and J. P. Murray, *Rev. Inorg. Chem.*, 1993, **13**, 125.
- J. P. Murray, K. J. Cavell and J. O. Hill, *Thermochim. Acta*, 1980, **36**, 97.
- M. A. V. Ribeiro da Silva and M. L. C. C. H. Ferrao, *J. Chem. Thermodyn.*, 1994, **26**, 315.
- R. Sabbah, D. Tabet, S. Belaadi, *Thermochim. Acta*, 1994, **247**, 193.
- L. A. Torres-Gomez, G. Barreiro-Rodriguez, and A. Galarza-Mondragon, *Thermochim. Acta*, 1988, **124**, 229.

6.3 13-15 (III-V) Semiconductor Chemical Vapor Deposition

6.3.1 Phosphine and Arsine³

Because of their use in metal organic chemical vapor deposition (MOCVD) of 13-15 (III-V) semiconductor compounds phosphine (PH_3) and arsine (AsH_3) are prepared on an industrial scale.

6.3.1.1 Synthesis

Phosphine (PH_3) is prepared by the reaction of elemental phosphorus (P_4) with water, (6.7). Ultra pure phosphine that is used by the electronics industry is prepared by the thermal disproportionation of phosphorous acid, (6.8).



Arsine can be prepared by the reduction of the chloride, (6.9) or (6.10). The corresponding syntheses can also be used for stibine and bismuthine.



The hydrolysis of calcium phosphide or arsenide can also generate the trihydrides.

³This content is available online at <<http://cnx.org/content/m33043/1.5/>>.

6.3.1.2 Structure

The phosphorus in phosphine adopts sp^3 hybridization, and thus phosphine has an umbrella structure (Figure 6.8a) due to the stereochemically active lone pair. The barrier to inversion of the umbrella ($E_a = 155$ kJ/mol) is much higher than that in ammonia ($E_a = 24$ kJ/mol). Putting this difference in context, ammonia's inversion rate is 10^{11} while that of phosphine is 10^3 . As a consequence it is possible to isolate chiral organophosphines (PRR'R''). Arsine adopts the analogous structure (Figure 6.8b).

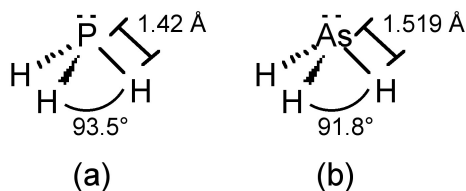


Figure 6.8: The structures of (a) phosphine and (b) arsine.

6.3.1.3 Reactions

Phosphine is only slightly soluble in water (31.2 mg/100 mL) but it is readily soluble in non-polar solvents. Phosphine acts as neither an acid nor a base in water; however, proton exchange proceeds via the phosphonium ion (PH_4^+) in acidic solutions and via PH_2^- at high pH, with equilibrium constants $K_b = 4 \times 10^{-28}$ and $K_a = 41.6 \times 10^{-29}$, respectively.

Arsine has similar solubility in water to that of phosphine (i.e., 70 mg/100 mL), and AsH_3 is generally considered non-basic, but it can be protonated by superacids to give isolable salts of AsH_4^+ . Arsine is readily oxidized in air, (6.11).



Arsine will react violently in presence of strong oxidizing agents, such as potassium permanganate, sodium hypochlorite or nitric acid. Arsine decomposes to its constituent elements upon heating to 250 - 300 °C.

6.3.1.3.1 Gutzeit test

The Gutzeit test is the characteristic test for arsenic and involves the reaction of arsine with Ag^+ . Arsine is generated by reduction of aqueous arsenic compounds, typically arsenites, with Zn in the presence of H_2SO_4 . The evolved gaseous AsH_3 is then exposed to silver nitrate either as powder or as a solution. With solid AgNO_3 , AsH_3 reacts to produce yellow Ag_4AsNO_3 , while with a solution of AgNO_3 black Ag_3As is formed.

6.3.1.4 Hazards

Pure phosphine is odorless, but technical grade phosphine has a highly unpleasant odor like garlic or rotting fish, due to the presence of substituted phosphine and diphosphine (P_2H_4). The presence of P_2H_4 also causes spontaneous combustion in air. Phosphine is highly toxic; symptoms include pain in the chest, a sensation of coldness, vertigo, shortness of breath, and at higher concentrations lung damage, convulsions and death. The recommended limit (RL) is 0.3 ppm.

Arsine is a colorless odorless gas that is highly toxic by inhalation. Owing to oxidation by air it is possible to smell a slight, garlic-like scent when arsine is present at about 0.5 ppm. Arsine attacks hemoglobin in the red blood cells, causing them to be destroyed by the body. Further damage is caused to the kidney and liver. Exposure to arsine concentrations of 250 ppm is rapidly fatal: concentrations of 25 – 30 ppm are fatal for 30 min exposure, and concentrations of 10 ppm can be fatal at longer exposure times. Symptoms of poisoning appear after exposure to concentrations of 0.5 ppm and the recommended limit (RL) is as low as 0.05 ppm.

6.3.1.5 Bibliography

- R. Minkwitz, A. Kornath, W. Sawodny, and H. Härtner, *Z. Anorg. Allg. Chem.*, 1994, **620**, 753.

6.3.2 Mechanism of the Metal Organic Chemical Vapor Deposition of Gallium Arsenide⁴

6.3.2.1 Introduction

Preparation of epitaxial thin films of III-V (13-15) compound semiconductors (notably GaAs) for applications in advanced electronic devices became a realistic technology through the development of metal organic chemical vapor deposition (MOCVD) processes and techniques. The processes mainly involves the thermal decomposition of metal alkyls and/or metal hydrides.

In 1968 Manasevit at the Rockwell Corporation was the first to publish on MOCVD for the epitaxial growth of GaAs. This followed his pioneering work in 1963 with the epitaxial growth of silicon on sapphire. The first publication used triethylgallium [$\text{Ga}(\text{CH}_2\text{CH}_3)_3$] and arsine (AsH_3) in an open tube with hydrogen as the carrier gas. Manasevit actually coined the phrase MOCVD and since this seminal work there have been numerous attempts to improve and expand MOCVD for the fabrication of GaAs.

Several processes, partly in series, partly in parallel take place during the growth by CVD. They are presented schematically in Figure 6.9. The relative importance of each of them depends on the chemical nature of the species involved and the design of the reactor used. The actual growth rate is determined by the slowest process in the series of events needed to come to deposition.

⁴This content is available online at <<http://cnx.org/content/m25614/1.6/>>.

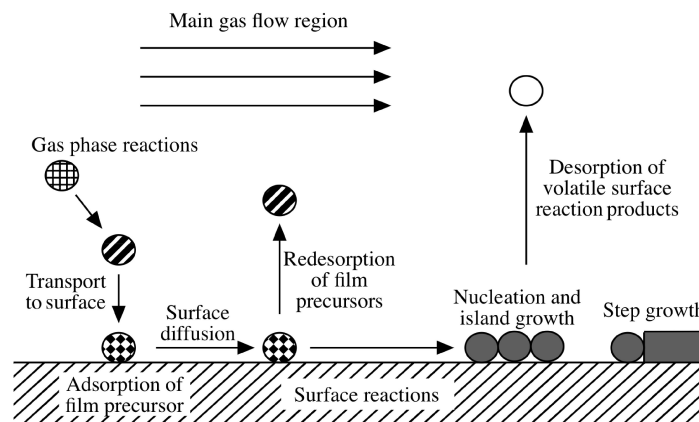


Figure 6.9: Schematic representation of the fundamental transport and reaction steps underlying MOCVD. Adapted from K. F. Jensen and W. Kern, in *Thin Film Processes II*, Eds. J. L. Vossen and W. Kern, Academic Press, New York (1991).

Conventionally, the metal organic chemical vapor deposition (MOCVD) growth of GaAs involves the pyrolysis of a vapor phase mixture of arsine and, most commonly, trimethylgallium [Ga(CH₃)₃, TMG] and triethylgallium [Ga(CH₂CH₃)₃, TEG]. Traditionally, growth is carried out in a cold-wall quartz reactor in flowing H₂ at atmospheric or low pressure. The substrate is heated to temperatures 400 - 800 °C, typically by RF heating of a graphite susceptor. Transport of the metal-organics to the growth zone is achieved by bubbling a carrier gas (e.g., H₂) through the liquid sources that are in held temperature-controlled bubblers.

6.3.2.2 Reaction mechanism

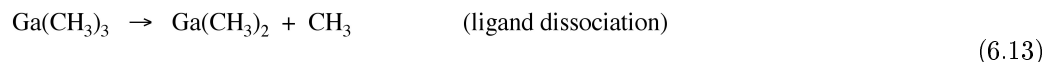
While the overall reaction (where R = CH₃ or CH₂CH₃) can be described by (6.12).

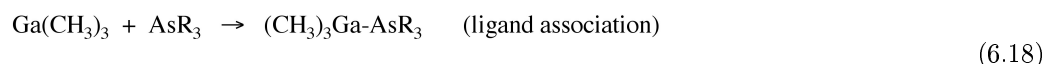
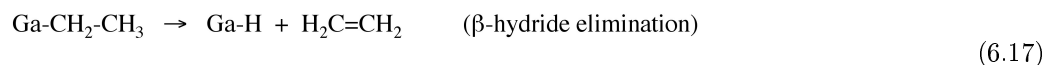
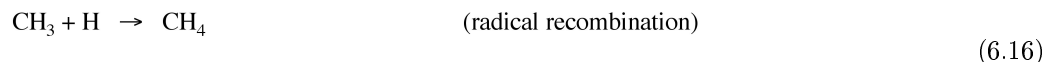
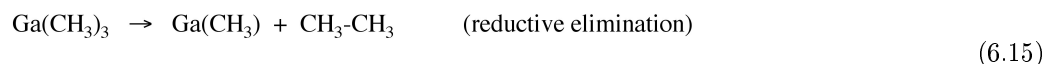
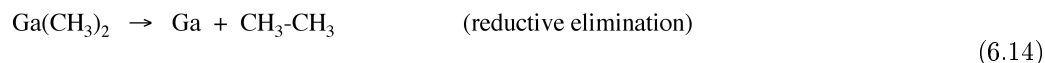


The nature of the reaction is much more complex. From early studies it was thought that free Ga atoms are formed by pyrolysis of TMG and As₄ molecules are formed by pyrolysis of AsH₃ and these species recombine on the substrate surface in an irreversible reaction to form GaAs.

Although a Lewis acid-base complex formed between TMG and AsH₃ is possible, it is now known that if there is any intermediate reaction between the TMG and AsH₃, the product is unstable. However, early work indicated that free GaAs molecules resulted from the decomposition of a TMG.AsH₃ intermediate and that the heated surface contributed to the reaction. It was subsequently suggested that the reaction occurs by separate pyrolysis of the reactants and a combination of individual Ga and As atoms at the surface or just above it. Finally, evidence has also been found for TMG pyrolysis followed by diffusion through a boundary layer and for AsH₃ pyrolysis catalyzed by the GaAs surface.

There are several different kinds of potential reactions occurring in the CVD reaction chamber, namely, ligand dissociation, ligand association, reductive elimination, oxidative addition, β-hydride elimination, etc. Some of them are listed in the following equations:





6.3.2.2.1 Using ALE studies as insight for MOCVD

Given the stepwise and presumably simplified mechanism for atomic layer epitaxy (ALE) growth of GaAs, a number of mechanistic studies have been undertaken of ALE using TMG and AsH₃ to provide insight into the comparable MOCVD reactions. Nishizawa and Kurabayashi proposed that a CH₃-terminated GaAs surface inhibits further heterogeneous decomposition of TMG and self-limits the growth rate to one monolayer/cycle. While, X-ray photoelectron spectroscopy (XPS) studies showed that no carbon was observed on a GaAs surface reacted with TMG. Furthermore, the same self-limiting growth was seen in ALE using a metalorganic molecular beam epitaxy (MOMBE) with TMG and AsH₃. It was reported that a transient surface reconstruction is observable by reflection high-energy electron diffraction (RHEED) during the ALE of GaAs in MOMBE. It was suggested that this structure is caused by CH₃-termination and the self-limitation of the growth rate is attributed to this structure. However, measurement of the desorption of CH₃ by means of a combination of pulsed molecular beams and time-resolved mass spectrometry, indicates that CH₃ desorption is too fast to attribute the self-limitation to the CH₃-terminated surface. Subsequently, investigations of the pyrolysis of TMG on a (100)GaAs surface by the surface photo-absorption method (SPA) allowed for the direct observation of CH₃ desorption from a GaAs surface reacted with TMG. From the measured CH₃ desorption kinetics, it was shown that the CH₃-terminated surfaces causes the self-limitation of the growth rate in ALE because the excess TMG cannot adsorb.

All this research helped people to visualize the real reaction mechanism in the formation of GaAs by MOCVD methods, in which the decomposition, diffusion and surface reaction interact with each other and result in a much more complicated reaction mechanism.

6.3.2.2.2 Gas phase reaction: pyrolysis of TMG and AsH₃

In the TMG/H₂ system, there is almost no reactions at a temperature below 450 °C, whereas the reaction of TMG with H₂ almost completely changed into CH₄ and Ga at a temperature above 600 °C, (6.19).



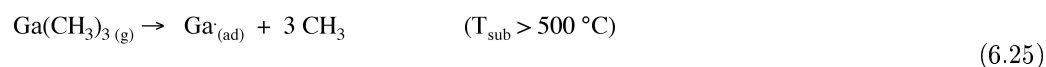
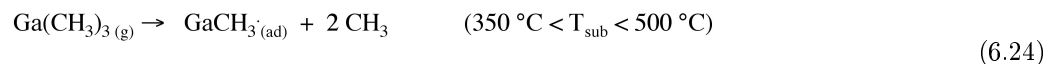
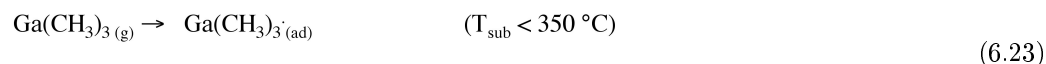
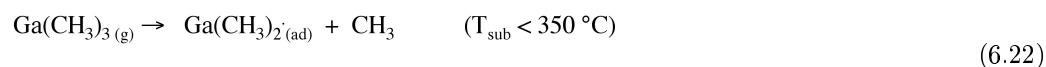
As for the AsH₃ decomposition, without any deposition of Ga or GaAs in the reactor, the pyrolysis of AsH₃ proceeded barely at a temperature below 600 °C, however, it proceeded nearly completely at a temperature above 750 °C. In the AsH₃/H₂ system with the TMG introduced previously, the decomposition of AsH₃ was largely enhanced even at a temperature below 600 °C. The decomposition of AsH₃ seems to be affected

sensitively by the deposited GaAs or Ga. This phenomenon may be concluded to be caused by the catalytic action by GaAs or Ga. The reaction at a temperature below 600 °C can be described as shown in (6.20), but at a temperature above 600 °C, pyrolysis of AsH₃ can occur even without GaAs or Ga, (6.21).

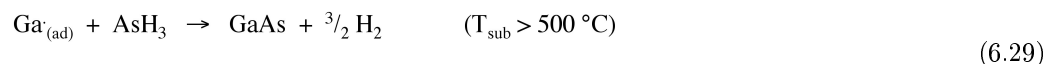
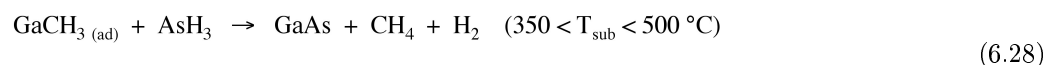
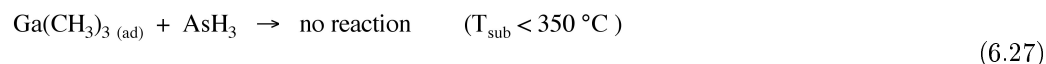
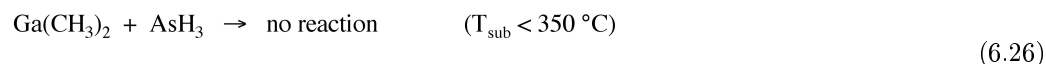


6.3.2.2.3 Adsorption and surface reactions

From the temperature dependent measurements of the desorption spectrum from a surface on which TMG was supplied, it was estimated that the surface-adsorbed species was Ga at the high temperature region of $T_{\text{sub}} > 500$ °C, GaCH₃ at the range of 350 °C $< T_{\text{sub}} < 500$ °C, and Ga(CH₃)₂ and Ga(CH₃)₃ at the range of $T_{\text{sub}} < 350$ °C. The reactions, where (ad) means the adsorbed state of the molecules, are:



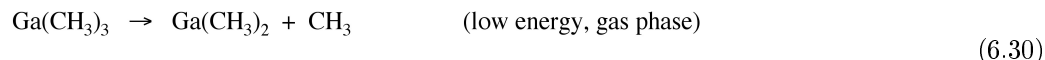
When AsH₃ is supplied, the reactions with these adsorbates are:



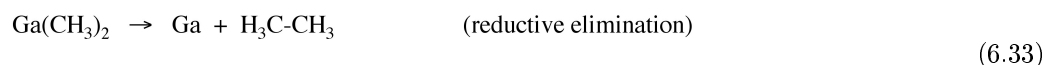
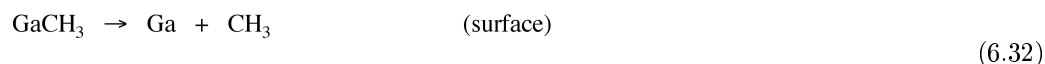
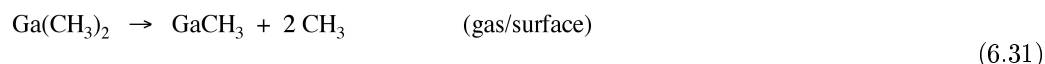
It was observed that there is no growth in the range of $T_{\text{sub}} < 350$ °C, i.e., Ga(CH₃)₂(ad) and Ga(CH₃)₃(ad) do not react with AsH₃ in the TMG-AsH₃ system. Monomolecular layer growth is limited by the formation of GaCH₃ and its reaction with AsH₃.

6.3.2.2.4 Overall reaction pathway

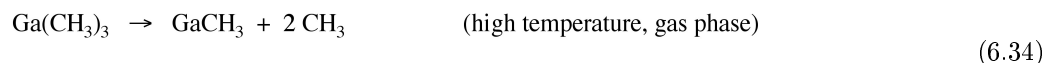
At lower temperature (350 - 500 °C), equivalently low energy, TMG decompose in the gas phase to Ga(CH₃)₂ and methyl radical, (6.30).



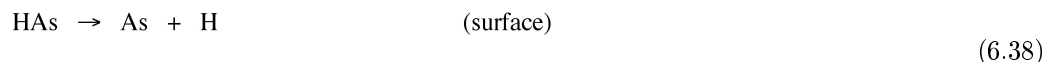
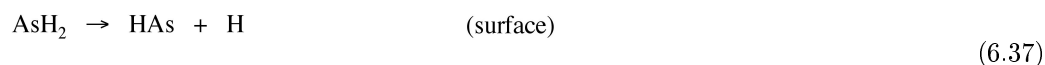
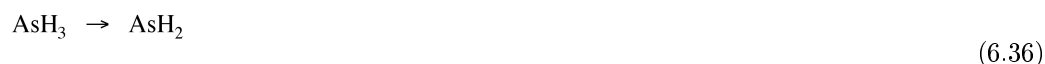
After the first ligand dissociation, there are two different pathways, in the first, the Ga(CH₃)₂ keeps decomposing into GaCH₃ and another methyl group when it is at the gas-substrate interface, (6.31), and then further decomposes into free gallium atoms on the substrate surface, (6.32). In the second reaction, the Ga(CH₃)₂ decomposes directly into Ga and CH₃-CH₃ by reductive elimination, (6.33).



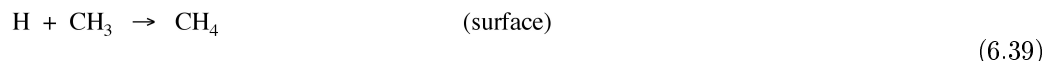
At high temperature (> 500 °C), the TMG decomposes into Ga(CH₃) and two methyl groups instead of the step-wise decomposition at lower temperature, (6.34), and the Ga(CH₃) further decomposes into free Ga atoms at the substrate surface, (6.35).



The decomposition of AsH₃ forms an “arsenic cloud” in the reaction chamber. The decomposition is also step-wise:



The methyl groups in the surface Ga(CH₃) molecules are removed by the formation of methane with atomic hydrogen from the decomposition of AsH₃, (6.39).



6.3.2.2.5 Kinetics for other systems

Investigations have been reported for the mechanism of the growth of GaAs using triethylgallium [Ga(CH₂CH₃)₃, TEG] and TMG with trimethylarsene [As(CH₃)₃, TMA], triethylarsene [As(CH₂CH₃)₃, TEA], *tert*-butylarsine {[(CH₃)₃C]AsH₂, TBA}, and phenylarsine [(C₆H₅)AsH₂]. The experiments were conducted in a MOCVD reactor equipped with a recording microbalance for in-situ growth rate measurements. For example, the kinetics of the growth of GaAs were investigated by measuring growth rate as a function of temperature using the microbalance reactor while holding the partial pressure of gallium precursor (e.g., TMG) and arsenic precursor [e.g., As(CH₃)₃] constant at 0.01 and 0.05 Torr, respectively. Three different flow rates were used to determine the influence of the gas residence time.

The growth rate of GaAs with TMG and As(CH₂CH₃)₃ is higher as compared with the growth from TMG and As(CH₃)₃ because of the lower thermal stability of As(CH₂CH₃)₃ than As(CH₃)₃. Both of the two growth rates showed a strong dependence on the residence time.

Similarly, the kinetic behaviors of the TMG/TBA and TEG/TBA system were investigated under the same conditions as the TMA and TEA studies. There are two distinct regions of growth. For TMG/TBA, the deposition rate is independent at low temperature and in the intermediate temperature (around 600 °C) the dependence of the growth rate on the total flow rate is significant. This means that the growth at the lower temperature is controlled by surface reactions. The TEG/TBA system showed a similar behavior except that the maximum growth rate occurs around 450 °C while it is around 750 °C for TMG/TBA system. Also, the growth of TMG/(C₆H₅)AsH₂ was studied on the same conditions as for the Me₃Ga/^tBuAsH₂ system. It was reported that the difference in the growth rate at various flow rates was related to a combination of parasitic reactions and depletion effects from deposition. From the comparison of the data, it is deduced that the effect of parasitic reactions is slightly smaller for (C₆H₅)AsH₂ than for TBA.

Two possible mechanisms for the dependence of growth rate on flow rate were proposed. The first, mass-transfer limitation was thought to be unlikely because of the high diffusivity of the gallium precursors at 1 Torr (ca. 350 cm²/s). The second, also the more likely explanation for the observed growth-rate dependence on flow rates is gas-phase depletion cause by the parasitic reactions. Since the growth efficiency is high (41% at 700 °C), the loss of precursor from the gas phase will directly affect the growth rate. It was evidenced by the differences in the growth rates between split and combined feed streams. The growth rate is lower when the reagents are combined upstream of the reactor than when they are combined inside the reactor (split stream). It is suggested that the experimental observations can be explained by a model based on the reversible formation of an adduct and the decomposition of this adduct to useless polymeric material competing with the growth of GaAs. It can be written in the form shown in (6.40) where k_f and k_r are the forward and reverse rate constants for adduct formation, respectively, k_d is the rate constant for the irreversible decomposition of the adduct to polymer, and k_s is the surface reaction rate constant for the growth of GaAs. It is obvious that each step involves several elementary reactions, but there were insufficient data to provide any more detail.



6.3.2.3 Bibliography

- T. H. Chiu, *Appl. Phys. Lett.*, 1989, **55**, 1244.
- H. Ishii, H. Ohno, K. Matsuzaki and H. Hasegawa, *J. Cryst. Growth*, 1989, **95**, 132.
- K. F. Jensen and W. Kern, in *Thin Film Processes II*, Eds. J. L. Vossen and W. Kern, Academic Press, New York (1991).
- N. Kobayashi, Y. Yamauchi, and Y. Horikoshi, *J. Cryst. Growth*, 1991, **115**, 353.
- K. Kodama, M. Ozeki, K. Mochizuki, and N. Ohtsuka, *Appl. Phys. Lett.*, 1989, **54**, 656.
- M. R. Leys and H. Veenvliet, *J. Cryst. Growth*, 1981, **55**, 145.
- U. Memmert and M. L. Yu, *Appl. Phys. Lett.*, 1990, **56**, 1883.

- J. Nishizawa and T. Kurabayashi, *J. Cryst. Growth*, 1988, **93**, 132.
- T. R. Omstead and K. F. Jensen, *Chem. Mater.*, 1990, **2**, 39.
- D. J. Schyer and M. A. Ring, *J. Electrochem. Soc.*, 1977, **124**, 569.
- Watanabe, T. Isu, M. Hata, T. Kamijoh, and Y. Katayama, *Japan. J. Appl. Phys.*, 1989, **28**, L1080.
- Y. Zhang, Th. Beuermann, and M. Stuke, *Appl. Phys. B*, 1989, **48**, 97.
- Y. Zhang, W. M. Cleaver, M. Stuke, and A. R. Barron, *Appl. Phys. A*, 1992, **55**, 261.

6.4 Oxide Chemical Vapor Deposition

6.4.1 Chemical Vapor Deposition of Silica Thin Films⁵

6.4.1.1 General considerations

Before describing individual chemical vapor deposition (CVD) systems for the deposition of silica thin films, it is worth outlining general considerations to be taken into account with regard to the growth by CVD of any insulating film: the type of CVD method, deposition variables, and limitations of the precursor.

6.4.1.1.1 Deposition methods

In regard to the CVD of insulating films in general, and silica films in particular, three general reactors are presently used: atmospheric pressure CVD (APCVD), low and medium temperature low pressure CVD (LPCVD), and plasma-enhanced CVD (PECVD). LPCVD is often further divided into low and high temperatures.

APCVD systems allow for high throughput and even continuous operation, while LPCVD provides for superior conformal step coverage and better film homogeneity. PECVD has been traditionally used where low temperatures are required, however, film quality is often poor. As compared to PECVD, photo-assisted CVD has the additional advantage of highly selective deposition, although it has been little used in commercial systems. Table 6.3 summarizes the advantages and disadvantages of each type of CVD system commercially used for SiO₂ films.

	Atmospheric pressure CVD	Low temperature LPCVD	Medium temperature LPCVD	Plasma enhanced CVD
Temperature (°C)	300 - 500	300 - 500	500 - 900	100 - 350
Throughput	high	high	high	low
Step coverage	poor	poor	conformal	poor
Film properties	good	good	excellent	poor
Uses	passivation, insulation	passivation, insulation	insulation	passivation, insulation

Table 6.3: Comparison of different deposition methods for SiO₂ thin films.

6.4.1.1.2 Deposition variables

The requirements of CVD films for electronic device applications have become increasingly more stringent as device sizes are continually reduced. Film thickness must be uniform across an entire wafer, i.e., better

⁵This content is available online at <<http://cnx.org/content/m24897/1.4/>>.

than $\pm 1\%$. The structure of the film and its composition must be controlled and reproducible, both on a single wafer, as well as between wafer samples. It is also desirable that the process is safe, inexpensive, and easily automated.

A number of variables determine the quality and rate of film growth for any material. In general, the deposition rate increases with increased temperature and follows the Arrhenius equation, (6.41), where R is the deposition rate, E_a is the activation energy, T is the temperature (K), A is the frequency factor, and k is Boltzmann's constant (1.381×10^{-23} J/K).

$$R = A \exp(-E_a/kT) \quad (6.41)$$

At the high temperatures the rate of deposition becomes mass transport limited. Meaning, the rate of surface reaction is faster than the rate at which precursors are transported to the surface. In multiple source systems, the film growth rate is dependent on the vapor phase concentration (or partial pressure) of each of the reactants, but in certain cases the ratio of reactants is also important, e.g., the SiH_4/O_2 growth of SiO_2 . Surface catalyzed reactions can also alter the deposition rate. Such as the non-linear dependence of the deposition rate of SiO_2 on the partial pressure of $\text{Si}(\text{OEt})_4$. Gas depletion may also be significant requiring either a thermal ramp in the chamber and/or special reactor designs. The necessary incorporation of dopants usually lowers deposition rates, due to competitive surface binding.

For the applications of insulating materials as isolation layers, an important consideration is step coverage: whether a coating is uniform with respect to the surface. Figure 6.10a shows a schematic of a completely uniform or conformal step coverage of a trench (such as occurs between isolated devices) where the film thickness along the walls is the same as the film thickness at the bottom of the step. Uniform step coverage results when reactants or reactive intermediates are able to migrate rapidly along the surface before reacting. When the reactants adsorb and react without significant surface migration, deposition is dependent on the mean free path of the gas. Figure 6.10b shows an example of minimal surface migration and a short mean free path. For SiO_2 film growth LPCVD has highly uniform coverage (Figure 6.10a) and PECVD poor step coverage (Figure 6.10b).

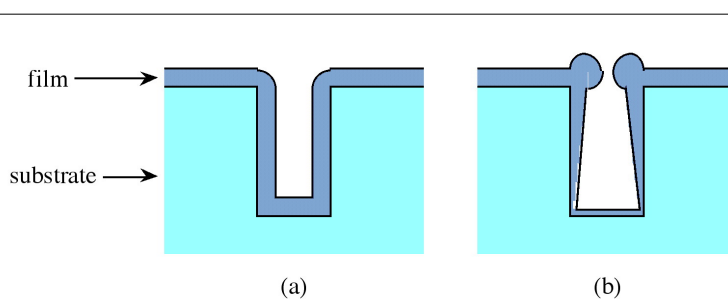


Figure 6.10: Step coverage of deposited films with (a) uniform coverage resulting from rapid surface migration and (b) nonconformal step coverage due to no surface migration.

6.4.1.1.3 Precursor considerations

The general requirements for any CVD precursor have been adequately reviewed elsewhere, and will not be covered here. However, many of the gases and organometallics used to deposit dielectric films are hazardous. The safety problems are more severe for LPCVD because the process often uses no diluent gas such as argon or nitrogen. Table 6.4 lists the boiling point and hazards of common inorganic and organometallic precursor

sources for CVD of SiO₂ and doped silica. Many of the precursors react with air to form solid products, thus leaks can cause particles to form in the chamber and gas lines.

Gas	Formula	Bpt (°C)	Hazard
ammonia	NH ₃	-33.35	toxic, corrosive
argon	Ar	-185.7	inert
arsine	AsH ₃	-55	toxic
diborane	B ₂ H ₆	-92.5	toxic, flammable
dichlorosilane	SiCl ₂ H ₂	8.3	toxic, flammable
hydrogen	H ₂	-252.8	flammable
nitrogen	N ₂	-209.86	inert
nitrous oxide	N ₂ O	-88.5	oxidizer
oxygen	O ₂	-182.962	oxidizer
phosphine	PH ₃	-87.7	toxic, P ₂ H ₄ impurities, flammable
silane	SiH ₄	-111.8	flammable, toxic

Table 6.4: Physical and hazard properties of common gaseous sources for CVD of dielectric materials.

In principle, the deposition of a SiO₂, or silica, thin film by CVD requires two chemical sources: the element (or elements) in question, and an oxygen source. While dioxygen (O₂) is suitable for many applications, its reactions may be too fast or too slow for optimum film growth, requiring that alternative oxygen sources be used, e.g., nitrous oxide (N₂O) and ozone (O₃). A common non-oxidizing oxygen source is water. A more advantageous approach is to incorporate oxygen into the ligand environment of the precursor, and endeavor to preserve such an interaction intact from the source molecule into the ultimate film; such a source is often termed a "single-source" precursor.

6.4.1.2 CVD silica (SiO₂)

The processing sequence for silicon dioxide (SiO₂) used depends on its specific use. CVD processes for SiO₂ films can be characterized by either the chemical reaction type, the growth pressure, or the deposition temperature. The choice of route is often dictated by requirements of the thermal stability of the substrate or the conformality. Table 6.5 summarizes selected properties of SiO₂ grown by various CVD methods, in comparison to that of thermally grown silica. In general, silica grown at high temperatures resemble thermally grown "native" SiO₂. However, the use of aluminum metallization requires low temperature deposition of silica.

Deposition	Plasma	SiH ₄ + O ₂	Si(OEt) ₄	SiCl ₂ H ₂ + N ₂ O	Thermal
Temperature (°C)	200	450	700	900	1000
Composition	SiO _{1.9} (H)	SiO ₂ (H)	SiO ₂	SiO ₂ (Cl)	SiO ₂
Step coverage	non-conformal	non-conformal	conformal	conformal	conformal
Thermal stability	loses H	densifies	stable	loses Cl	stable
Refractive index	1.47	1.44	1.46	1.46	1.46
Dielectric constant	4.9	4.3	4.0	4.0	3.9

Table 6.5: Comparison of physical properties of SiO₂ grown by commercial CVD methods.

6.4.1.2.1 CVD from hydrides

The most widely used method for SiO₂ thin film CVD is the oxidation of silane (SiH₄), first developed in 1967 for APCVD. Nonetheless, LPCVD systems have since become increasingly employed, and exceptionally high growth rates (30,000 Å/min) have been obtained by the use of rapid thermal CVD.

The chemical reaction for SiO₂ deposition from SiH₄ is:



At high oxygen partial pressures an alternative reaction occurs, resulting in the formation of water.



While these reactions appear simple, the detailed mechanism involves a complex branching-chain sequence of reactions. The apparent activation energy is low (< 41 kJ/mol) as a consequence of its heterogeneous nature, and involves both surface adsorption and surface catalysis.

Nitrous oxide (N₂O) can be used as an alternative oxygen source to O₂, according to the overall reaction, (6.44).



A simple kinetic scheme has been developed to explain many of the observed aspects of SiH₄-N₂O growth. It was suggested that the reaction is initiated by decomposition of N₂O, (6.45), generating an oxygen radical which can abstract hydrogen from silane forming a hydroxyl radical, (6.46), that can react further with silane, (6.47).



Evidence for the reaction of the OH radical to form water is the formation of a small quantity of water observed during the oxidation of SiH₄. Silyl radicals are oxidized by N₂O to form siloxy radicals, (6.48), which provide a suitable propagation step, (6.49).



It has been proposed that the silanol (SiH₃OH) is the penultimate film precursor.

The SiH₄-O₂ and SiH₄-N₂O routes to SiO₂ thin films are perhaps the most widely studied photochemical CVD system of all dielectrics. Photo-CVD of SiO₂ provides a suitable route to deposition at low substrate temperatures, thereby avoiding potential thermal effects of wafer warpage and deleterious dopant redistribution. In addition, unlike other low temperature methods such as APCVD and PECVD, photo-CVD often provides good purity of films.

A summary of common silane CVD systems is given in Table 6.6.

Oxygen source	Carrier gas (diluent)	CVD method	Deposition temp. (°C)	Growth rate (Å/min)
O ₂	N ₂	APCVD	350 - 475	100 - 14,000
O ₂	Ar	LPCVD	100 - 550	100 - 30,000
O ₂	Ar/N ₂	LPCVD	25 - 500	10 - 450
O ₂	Ar	PECVD	25 - 200	200 - 900
N ₂ O	N ₂	APCVD	490 - 690	200 - 1,200
N ₂ O	N ₂	LPCVD	700 - 860	ca. 50
N ₂ O	N ₂	LPCVD	25 - 350	7 - 180
N ₂ O	Ar	PECVD	100 - 200	80 - 800

Table 6.6: Precursors and deposition conditions for SiO₂ CVD using silane (SiH₄).

6.4.1.2.2 CVD from halides

The most widely used process of the high temperature growth of SiO₂ by LPCVD involves the N₂O oxidation of dichlorosilane, SiCl₂H₂, (6.50).



Deposition at 900 - 915 °C allows for growth of SiO₂ films at ca. 120 Å/min; however, these films are contaminated with Cl. Addition of small amounts of O₂ is necessary to remove the chlorine.

While PECVD has been employed utility halide precursors, the ability of small quantities of fluorine to improve the electrical properties of SiO₂ has prompted investigation of the use of SiF₄ as a suitable source.

6.4.1.2.3 CVD from tetraethoxysilane (TEOS)

The first CVD process to be introduced into semiconductor technology in 1961 was that involving the pyrolysis of tetraethoxysilane, Si(OEt)₄ (commonly called TEOS from tetraethylorthosilicate). Deposition occurs at an optimum temperature around 750 °C. However, under LPCVD conditions, the growth temperature can be significantly lowered (> 600 °C). The high temperature growth of SiO₂ from TEOS involves no external oxygen source. Dissociative adsorption studies indicate that decomposition of the TEOS-derived surface bound di- and tri-ethoxysiloxanes is the direct source of the ethylene.

PECVD significantly lowers deposition temperatures using TEOS, but requires the addition of O₂ to remove carbon contamination, via the formation of gaseous CO and CO₂, which are subsequently not incorporated within the film. Although deposition as low as 100 °C may be obtained, the film resistivity increases by three orders of magnitude by depositing at 200 °C; being 10¹⁶ Ω.cm, with a breakdown strength of 7 x 10⁶ V/cm.

Addition of O₂ for APCVD growth does not decrease the deposition temperature, however, if ozone (O₃) is used as the oxidation source, deposition temperatures as low as 300 °C may be obtained for uniform crack-free films. It has been postulated that the ozone traps the TEOS molecule on the surface as it reacts with the ethoxy substituent, providing a lower energy pathway (TEOS-O₃ @ 55 kJ/mol versus TEOS-O₂ @ 230 kJ/mol and TEOS only @ 190 kJ/mol).

There are significant advantages of the TEOS/O₃ system, for example the superior step coverage it provides. Furthermore, films have low stress and low particle contamination. On this basis the TEOS/O₃ system has become widely used for silica, as well as silicate glasses.

6.4.1.2.4 CVD from other organosilicon precursors

A wide range of alternative silicon sources has been investigated, especially with regard to either lower temperature deposition and/or precursors with greater ambient stability.

Diethylsilane (Et_2SiH_2), 1,4-disilabutane (DBS, $\text{H}_3\text{SiCH}_2\text{CH}_2\text{SiH}_3$), 2,4,6,8-tetramethylcyclotetrasiloxane (TMCTS, Figure 6.11a, where $\text{R} = \text{CH}_3$), and 2,4,6,8-tetraethylcyclotetrasiloxane (TECTS, Figure 6.11a, where $\text{R} = \text{C}_2\text{H}_5$), have been used in conjunction with O_2 over deposition temperatures of 100 - 600 °C, depending on the precursor. Diacetoxydi-*tert*-butyl silane (DADBS, Figure 6.11b) has been used without additional oxidation sources. High quality silicon oxide has been grown at 300 °C by APCVD using the amido precursor, $\text{Si}(\text{NMe}_2)_4$ (Figure 6.11c).

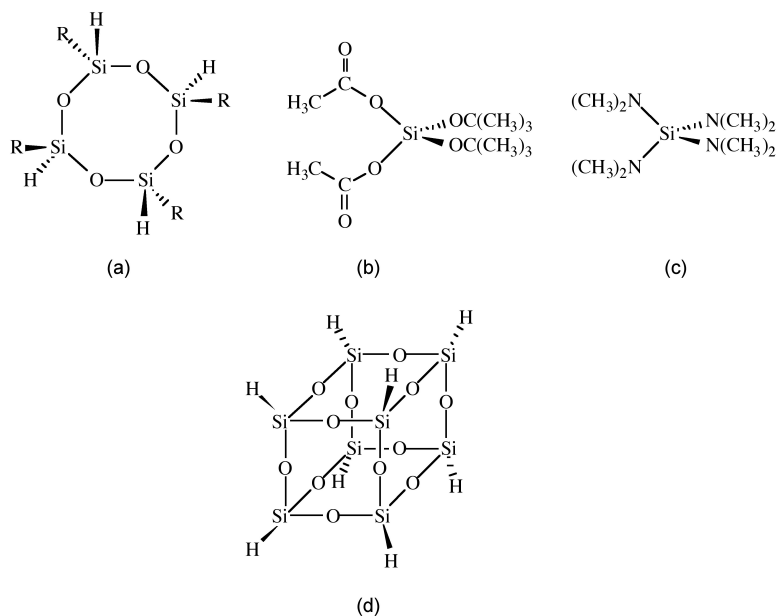


Figure 6.11: Alternative organometallic silicon sources that have been investigated for the growth of silica thin films.

An interesting concept has been to preform the -Si-O-Si- framework in the precursor. In this regard, the novel precursor T_8 -hydridospherosiloxane ($\text{H}_8\text{Si}_8\text{O}_{12}$, Figure 6.11d) gives smooth amorphous stoichiometric SiO_2 at 450 - 525 °C by LPCVD. The decomposition mechanism in the presence of added oxygen involves the loss of water, (6.51). IR studies indicate that the Si-O-Si bonds are preserved during deposition. While films are of high quality, the present synthesis of $\text{H}_8\text{Si}_8\text{O}_{12}$ is of low yield (ca. 21%), making it currently impractical for large scale processing.



6.4.1.3 CVD silicate glasses

Borosilicate glasses (BSG), phosphosilicate glasses (PSG) and borophosphosilicate glasses (BPSG) are frequently used as insulating layers separating conducting layers. These glasses have lower intrinsic stress, lower melting temperatures and better dielectric properties than SiO_2 itself. PSG and BPSG have the added property of gettering and immobilizing dopants. Particularly important is the gettering of sodium ions, which are a source of interface traps. The low temperature molten properties of BSG, PSG, and BPSG glasses allow for the smoothing of the device topography by viscous thermal fusion to convert abrupt steps to more gradually tapered steps (Figure 6.12a) as well as planarization of complex topologies (Figure 6.12b), enabling deposition of continuous metal layers. This process is commonly called P-glass flow. The boron and phosphorous contents of the silicate glasses vary, depending on the application, typically being from 2 to 8 weight per cent.

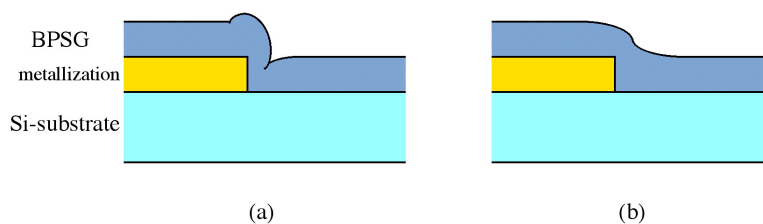


Figure 6.12: Schematic cross section of BPSG as deposited (a) and after annealing (b), showing the flow causing a decrease in the angle of the BPSG going over the step.

The advantage of BPSG over PSG is that flow occurs over the temperature range of 750 - 950 °C, depending on the relative P and B content (as opposed to 950 - 1110 °C for PSG). Lowering of the flow temperature is required to minimize dopant migration in VLSI devices. Conversely, the disadvantages of BPSG versus PSG include the formation of bubbles of volatile phosphorous oxides and crystallites of boron-rich phases. If, however, the dopant concentration is controlled, these effects can be minimized.

Arsenosilicates (AsSG) were employed originally in silicon device technology as an arsenic dopant source for planar substrates prior to the advent of large scale ion implantation which has largely removed the need for AsSG in doping applications. However, with ULSI silicon circuit fabrication, the requirement for doping of deep trenches (inaccessible to ion implantation) has witnessed the re-emergence of interest in AsSG films.

The CVD growth of silicate glasses follows that of SiO_2 , with SiH_4 and TEOS being the most commonly employed silicon precursors. A summary of common CVD precursor systems for silicate glasses is given in Table 6.7.

Precursors	CVD method	Deposition temp. (°C)	Applications
SiH ₄ /B ₂ H ₆	APCVD	300 - 450	good step coverage
SiH ₄ /B ₂ H ₆	LPCVD	350 - 400	-
SiH ₄ /PH ₃	APCVD	300 - 450	-
SiH ₄ /PH ₃	LPCVD	350 - 400	flow glass
SiH ₄ /B ₂ H ₆ /PH ₃	APCVD	300 - 450	-
SiH ₄ /B ₂ H ₆ /PH ₃	LPCVD	350 - 400	-
SiH ₄ /AsH ₃	APCVD	500 - 700	-
TEOS/B(OMe) ₃	APCVD	650 - 730	diffusion source
TEOS/B(OMe) ₃	LPCVD	500 - 750	trench filling
TEOS/B(OEt) ₃	APCVD	475 - 800	diffusion source
TEOS/B(OEt) ₃	LPCVD	500 - 750	diffusion source
TEOS/PH ₃	LPCVD	650	flow glass
TEOS/O=P(OMe) ₃	APCVD	300 - 800	flow glass
TEOS/P(OMe) ₃	LPCVD	500 - 750	diffusion source
TEOS/O=P(OMe) ₃	LPCVD	500 - 800	flow glass
TEOS/B(OMe) ₃ /PH ₃	LPCVD	620 - 800	trench filling
TEOS/B(OMe) ₃ /P(OMe) ₃	LPCVD	675 - 750	flow glass
TEOS/B(OMe) ₃ /O=P(OMe) ₃	LPCVD	680	flow glass
TEOS/AsCl ₃	APCVD	500 - 700	diffusion source
TEOS/As(OEt) ₃	LPCVD	700 - 730	trench doping
TEOS/O=As(OEt) ₃	LPCVD	700 - 730	trench doping

Table 6.7: Precursors and deposition conditions for CVD of borosilicate glass (BSG), phososilicate glass (PSG), borophosphosilicate glass (BPSG) and arsenosilicates (AsSG) thin films.

6.4.1.3.1 CVD from hydrides

Films of BSG, PSG, and BPSG may all be grown from SiH₄, O₂ and B₂H₆ and/or PH₃, at 300 - 650 °C. For APCVD, the reactants are diluted with an inert gas such as nitrogen, and the O₂/hydride molar ratio is carefully controlled to maximize growth rate and dopant concentration (values of 1 to 100 are used depending on the application). Ordinarily, the dopant concentration for both BSG and PSG decreases with increased temperature. However, some reports indicate an increase in boron content with increased temperature. Film growth of BPSG was found to occur in two temperature regions. Deposition at low temperature (270 - 360 °C) occurred via a surface reaction rate limiting growth ($E_a = 39$ kcal/mol), while at higher temperature (350 - 450 °C), a mass-transport rate limited reaction region is observed ($E_a = 7.6$ kcal/mol).

LPCVD of BSG and PSG is conducted at 450 - 550 °C with an O₂:hydride ratio of 1:1.5. Conversely, an O₂:hydride ratio of 1.5:1 provides the optimum growth conditions for BPSG over the same temperature range. The phosphorous in PSG films was found to exist as a mixture of P₂O₅ and P₂O₃, however, the latter can be minimized under the correct deposition conditions. Some difficulties have been reported for the use of B₂H₆ due to its thermal instability. Substitution of B₂H₆ with BCl₃ obviates this problem, although the resulting films are invariably contaminated with 1 weight per cent chloride.

Arsenosilicate glass (AsSG) thin films are generally grown by APCVD using arsine (AsH_3); the use of which is being limited due to its high toxicity. However, arsine inhibits the gas phase reactions between SiH_4 and O_2 , such that film grown from $\text{SiH}_4/\text{AsH}_3/\text{O}_2$ show improved step coverage at high deposition rates.

6.4.1.3.2 CVD from metal organic precursors

As with SiO_2 deposition, see above, there has been a trend towards the replacement of SiH_4 with TEOS on account of its ability to produce highly conformal coatings. This is particularly attractive with respect to trench filling. Furthermore, films of doped SiO_2 glasses have been obtained using both APCVD and LPCVD (typically below 3 Torr), with a wide variety of dopant elements including: boron, phosphorous, and arsenic, including antimony, tin, and zinc.

Boron-containing glasses are generally grown using either trimethylborate, $\text{B}(\text{OMe})_3$, or triethylborate, $\text{B}(\text{OEt})_3$, although the multi-element source, *tris*(trimethylsilyl)borate, $\text{B}(\text{OSiMe}_3)_3$, has been employed for both silicon and boron in BPSG thin film growth. Similarly, whereas PH_3 may be used as the phosphorous source, trimethylphosphite, $\text{P}(\text{OMe})_3$, and trimethylphosphate, $\text{O}=\text{P}(\text{OMe})_3$, are preferred. Likewise, triethoxyarsine, $\text{As}(\text{OEt})_3$, and triethylarsenate, $\text{O}=\text{As}(\text{OEt})_3$, have been employed for AsSG growth.

The co-reaction of TEOS with organoboron and organophosphorous compounds allows for deposition at lower temperatures (500 - 650 °C) than for hydride growth of comparable rates. However, LPCVD, using an all organometallic approach, requires $\text{P}(\text{OMe})_3$ because the low reactivity of $\text{O}=\text{P}(\text{OMe})_3$ prevents significant phosphorus incorporation. Although premature decomposition of $\text{P}(\text{OMe})_3$ occurs at 600 °C (leading to non-uniform growth), deposition at 550 °C results in high film uniformity at reasonable deposition rates.

6.4.1.4 Bibliography

- W. Kern and V. S. Ban, in *Thin Film Processes*, Eds. J. L. Vossen, W. Kern, Academic Press, New York (1978).
- M. L. Hammod, *Solid State Technol.*, 1980, **23**, 104.
- A. R. Barron and W. S. Rees, Jr., *Adv. Mater. Optics Electron.*, 1993, **2**, 271.
- N. Goldsmith and W. Kern, *RCA Rev.*, 1967, **28**, 153.
- C. Pavelescu, J. P. McVittie, C. Chang, K. C. Saraswat, and J. Y. Leong, *Thin Solid Films*, 1992, **217**, 68.
- J. D. Chapple-Sokol, C. J. Giunta, and R. G. Gordon, *J. Electrochem. Soc.*, 1987, **136**, 2993.
- P. González, D. Fernández, J. Pou, E. García, J. Serra, B. León, and M. Pérez-Amor, *Thin Solid Films*, 1992, **218**, 170.
- E. L. Jordan, *J. Electrochem. Soc.*, 1961, **108**, 478.
- K. Fujino, Y. Nishimoto, N. Tokumasu, and K. Maeda, *J. Electrochem. Soc.*, 1990, **137**, 2883.
- R. A. Levy and K. Nassau, *J. Electrochem. Soc.*, 1986, **133**, 1417.
- L. K. White, J. M. Shaw, W. A. Kurylo, and N. Miskowski, *J. Electrochem. Soc.*, 1990, **137**, 1501.

6.4.2 Chemical Vapor Deposition of Alumina⁶

6.4.2.1 Alumina

Alumina, Al_2O_3 , exists as multiple crystalline forms, however, the two most important are the α and γ forms. α - Al_2O_3 (corundum) is stable at high temperatures and its structure consists of a hexagonal close-packed array of oxide (O^{2-}) ions with the Al^{3+} ions occupying octahedral interstices. In contrast, γ - Al_2O_3 has a defect spinel structure, readily takes up water and dissolves in acid. Despite the potential disadvantages of γ - Al_2O_3 there is a preference for its deposition on silicon substrates because of the two different lattice-matching relationships of γ - Al_2O_3 (100) on Si(100). These are shown as schematic diagrams in Figure 6.13. A summary of CVD precursor systems for Al_2O_3 is given in Table 6.8.

⁶This content is available online at <<http://cnx.org/content/m24918/1.5/>>.

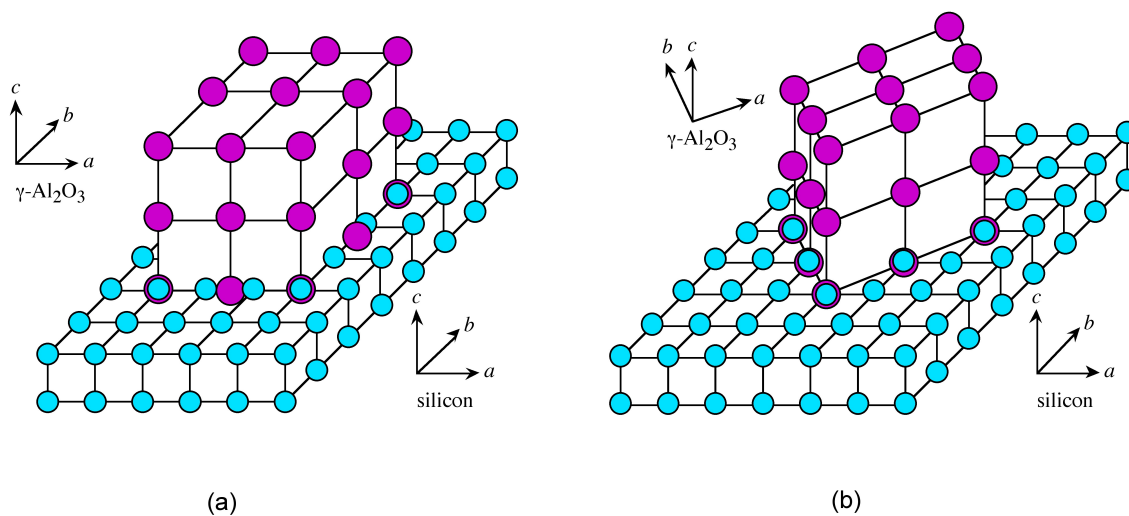


Figure 6.13: Schematic diagram of the crystallographic relations of $\gamma\text{-Al}_2\text{O}_3$ on Si(100): (a) $\gamma\text{-Al}_2\text{O}_3$ (100)||Si(100), and (b) $\gamma\text{-Al}_2\text{O}_3$ (100)||Si(110). Adapted from A. R. Barron, *CVD of Non-Metals*, W. S. Rees, Jr., Ed. VCH, New York (1996).

Aluminum precursor	Oxygen source	Carrier gas	CVD method	Deposition temp. ($^{\circ}\text{C}$)	Comments
AlCl_3	CO_2/H_2	H_2 or N_2	APCVD	700 - 900	amorphous (700), crystalline (850 - 900)
AlMe_3	O_2	N_2 or He	APCVD	350 - 380	dep. rate highly dependent on gas-phase conc. Al and O_2

continued on next page

AlMe ₃	O ₂	N ₂	LPCVD	375	plasma-enhanced, 10 W
AlMe ₃	N ₂ O	N ₂ or He	APCVD	100 - 660	lower quality than with O ₂
AlMe ₃	N ₂ O	N ₂	LPCVD	950 - 1050	good passivation properties of Si MOS devices
AlMe ₃	N ₂ O	He	PECVD	120 - 300	plasma-enhanced,
Al(O ⁱ Pr) ₃	O ₂	N ₂	APCVD	420 - 600	
Al(O ⁱ Pr) ₃	O ₂	N ₂	LPCVD	250 - 450	
Al(O ⁱ Pr) ₃	N ₂ O	Ar	LPCVD	200 - 750	epitaxial on Si
Al(acac) ₃		N ₂	APCVD	420 - 450	high C content
Al(acac) ₃	air	N ₂	APCVD	250 - 600	significant C content
Al(acac) ₃	O ₂ and H ₂ O	Ar	LPCVD	230 - 550	growth rate indep. of H ₂ O but film quality dep. on H ₂ O

Table 6.8: Precursors and deposition conditions for Al₂O₃ CVD.

6.4.2.1.1 CVD from halides

The initial use of CO₂/H₂ as a hydrolysis source for the CVD of SiO₂ from SiCl₄, led to the analogous deposition of Al₂O₃ from AlCl₃, i.e.,



Deposition in the temperature range 700 - 900 °C was found to yield films with optimum dielectric properties, but films deposited below 700 °C contained significant chloride impurities. It has been determined that H₂O vapor, formed from H₂ and CO₂, acts as the oxygen donor, and not the CO₂. The crystal form of the CVD-grown alumina films was found to depend on the deposition temperature; films grown below 900 °C were γ -Al₂O₃, while those grown at 1200 °C were α -Al₂O₃, in accord with the known phase diagram for this material.

6.4.2.1.2 CVD from trimethylaluminum (TMA)

Although trimethylaluminum, AlMe₃ (TMA), reacts rapidly with water to yield Al₂O₃, the reaction is highly exothermic (-1243 kJ/mol) and thus difficult to control. The oxygen gettering properties of aluminum metal, however, can be employed in the controlled MOCVD growth of Al₂O₃. The common deposition conditions employed for CVD of Al₂O₃ from AlMe₃ are similar to those used for aluminum-metal CVD, but with the addition of an oxygen source, either O₂ or N₂O.

Films grown by APCVD using N₂O are of inferior quality to those employing O₂, due to their exhibiting some optical absorption in the visible wavelength region. The growth of high quality films using either

oxygen source is highly dependent on the gas phase concentrations of aluminum and “oxygen”. Further improvements in film quality are observed with the use of a temperature gradient in the chambers deposition zone.

Attempts to lower the deposition temperature employing PECVD have been generally successful. However, a detailed spectroscopic study showed that the use of N_2O as the oxygen source resulted in significant carbon and hydrogen incorporation at low temperatures (120 - 300 °C). The carbon and hydrogen contamination are lowered at high deposition temperature, and completely removed by a post-deposition treatment under O_2 . It was proposed that the carbon incorporated in the films is in the chemical form of $Al-CH_3$ or $Al-C(O)OH$, while hydrogen exists as $Al-OH$ moieties within the film.

Photo-assisted CVD of Al_2O_3 from $AlMe_3$ has been reported to provide very high growth rates (2000 Å/min) and give films with electrical properties comparable to films deposited using thermal or plasma techniques. Irradiation with a 248 nm (KrF) laser source allowed for uniform deposition across a 3" wafer. However, use of 193 nm (ArF) irradiation required dilution of the $AlMe_3$ concentration to avoid non-uniform film growth.

6.4.2.1.3 CVD from alkoxides and β -diketonates

The pyrophoric nature of $AlMe_3$ urged investigations into alternative precursors, in particular those which already contain oxygen. Alternative precursors might also provide possible routes to eliminate carbon contamination. Given the successful use of TEOS in SiO_2 thin film growth, an analogous alkoxide precursor approach is logical. The first report of Al_2O_3 films grown by CVD used an aluminum alkoxide precursors.

Aluminum tris-*iso*-propoxide, $Al(O^iPr)_3$, is a commercially available inexpensive alkoxide precursor compound. Deposition may be carried-out by either APCVD or LPCVD, using oxygen as an additional oxidation source to ensure low carbon contamination. It is adventitious to use LPCVD (10 Torr) growth to inhibit gas phase homogeneous reactions, causing formation of a powdery deposit. The use of lower chamber pressures (3 Torr) and N_2O as the oxide source provided sufficient improvement in film quality to allow for device fabrication.

The deposition of Al_2O_3 films from the pyrolysis of aluminum acetylacetonate, $Al(acac)_3$ (Figure 6.14a), has been widely investigated using both APCVD and LPCVD. The perceived advantage of $Al(acac)_3$ over other aluminum precursors includes lowered-toxicity, good stability at room temperature, easy handling, high volatility at elevated temperatures, and low cost. However, the quality of films was originally poor; carbon being the main contaminant resulting from the thermolysis and incorporation of acetone and carbon dioxide formed upon thermal decomposition (Figure 6.15).

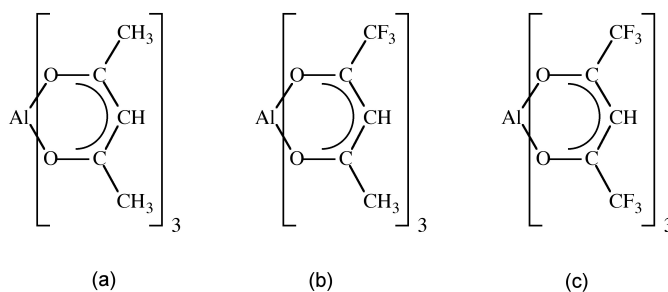


Figure 6.14: Aluminum β -diketonate precursors.

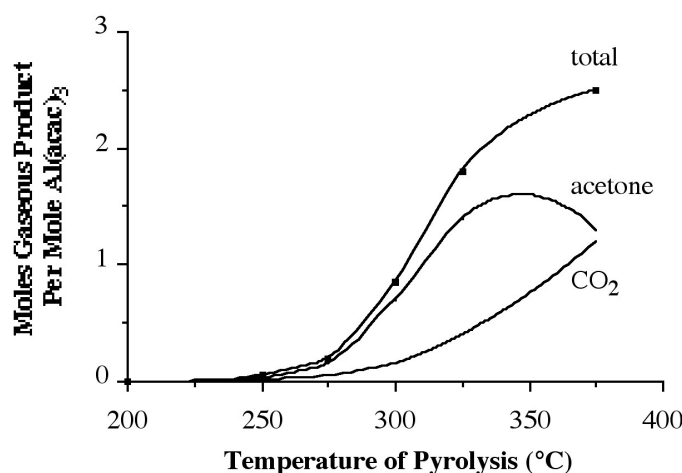


Figure 6.15: Gaseous decomposition products from the pyrolysis of $\text{Al}(\text{acac})_3$ as a function of pyrolysis temperature (Data from J. Von Hoene, R. G. Charles, and W. M. Hickam, *J. Phys. Chem.*, 1958, **62**, 1098).

Incomplete oxidation of the film may be readily solved by the addition of water vapor to the carrier gas stream; pure carbon-free films being grown at temperatures as low as 230 °C. In fact, water vapor plays an important role in the film growth kinetics, film purity, and the surface morphology of the grown films. While the growth rate is unaffected by the addition of water vapor, its influence on the surface morphology is significant. Films grown without water vapor on the Al_2O_3 surface is rough with particulates. In contrast, films grown with water vapor are mirror smooth.

A systematic study of the kinetics of vaporization of $\text{Al}(\text{acac})_3$ along with fluorinated aluminum β -diketonate complexes, $\text{Al}(\text{tfac})_3$ (Figure 6.14b) and $\text{Al}(\text{hfac})_3$ (Figure 6.14c), has been reported, and the saturation vapor pressures determined at 75 - 175 °C.

6.4.2.2 Aluminum silicates

The high dielectric constant, chemical stability and refractory character of aluminosilicates, $(\text{Al}_2\text{O}_3)_x(\text{SiO}_2)_y$, makes them useful as packaging materials in IC chip manufacture. Mullite ($3\text{Al}_2\text{O}_3 \cdot 2\text{SiO}_2$) prepared by sol-gel techniques, is often used as an encapsulant for active devices and thin-film components. Amorphous alumina-silica films have also been proposed as insulators in multilevel interconnections, since they do not suffer the temperature instability of alumina films retain the desirable insulating characteristics. Under certain conditions of growth and fabrication, silica may crystallize, thereby allowing diffusion of oxygen and impurities along grain boundaries to the silicon substrate underneath. Such unwanted reactions are catastrophic to the electronic properties of the device. The retention of amorphous structure over a larger temperature range of silicon rich alumina-silica films offers a possible solution to this deleterious diffusion.

Thin films of mixed metal oxides are usually obtained from a mixture of two different kinds of alkoxide precursors. However, this method suffers from problems with stoichiometry control since extensive efforts must be made to control the vapor phase concentration of two precursors with often dissimilar vapor pressures. Also of import here is the near impossible task of matching rates of hydrolysis/oxidation to give "pure", non-phase segregated films, i.e., those having a homogeneous composition and structure. In an effort

to solve these problems, research effort has been aimed at single-source precursors, i.e., those containing both aluminum and silicon.

The first study of single-source precursors for $(\text{Al}_2\text{O}_3)_x(\text{SiO}_2)_y$ films employed the mono-siloxide complex $\text{Al}(\text{O}^i\text{Pr})_2(\text{OSiMe}_3)$ (Figure 6.16a). However, it was found that except for deposition at very high temperatures ($> 900\text{ }^\circ\text{C}$) the deposited films this mono-siloxide compound were aluminum-rich ($\text{Al}/\text{Si} = 1.3 - 2.1$) and thus showed thermal instability in the insulating properties caused by crystallization in the films. It would appear that in order for silicon-rich alumina-silica films to be grown more siloxane substituents are required, e.g., the *tris*-siloxo aluminum complex $[\text{Al}(\text{OSiEt}_3)_3]_2$ (Figure 6.16b).

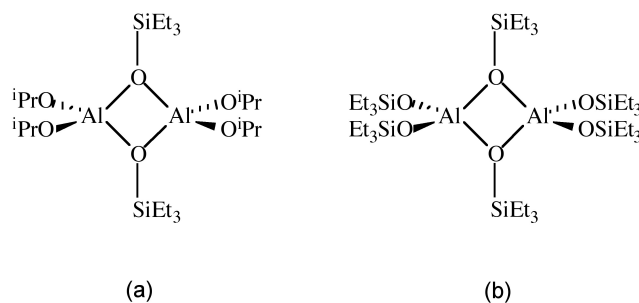


Figure 6.16: Precursors for aluminum silicate thin films.

The Al/Si ratio of thin films growth by APCVD using $[\text{Al}(\text{OSiEt}_3)_3]_2$ at $420 - 550\text{ }^\circ\text{C}$, was found to be dependent on the deposition temperature and the carrier gas composition (O_2/Ar). This temperature and oxygen-dependent variation in the film composition suggests that two competing precursor decomposition pathways are present.

1. Deposition in the absence of O_2 , is similar to that observed for the decomposition of $\text{Al}(\text{O}^i\text{Pr})_2(\text{OSiMe}_3)$ under N_2 , and would imply that the film composition is determined by the temperature-dependent tendencies of the Al-O-Si bonds to cleave.
2. The temperature-independent oxidative decomposition of the precursor. While it is possible to prepare films richer in Si using $[\text{Al}(\text{OSiEt}_3)_3]_2$ rather than $\text{Al}(\text{O}^i\text{Pr})_2(\text{OSiMe}_3)$, the Al:Si ratio is unfortunately not easily controlled simply by the number of siloxy ligands per aluminum in the precursor.

Films grown from the single-source precursor $\text{Al}(\text{O}^i\text{Pr})_2(\text{OSiMe}_3)$ crystallize to kyanite, Al_2SiO_5 , whereas those grown from $[\text{Al}(\text{OSiEt}_3)_3]_2$ remained amorphous even after annealing.

6.4.2.3 Bibliography

- A. W. Applett, L. K. Cheatham, and A. R. Barron, *J. Mater. Chem.*, 1991, **1**, 143.
- K. M. Gustin and R. G. Gordon, *J. Electronic Mater.*, 1988, **17**, 509.
- C. Landry, L. K. Cheatham, A. N. MacInnes, and A. R. Barron, *Adv. Mater. Optics Electron.*, 1992, **1**, 3.
- Y. Nakaido and S. Toyoshima, *J. Electrochem. Soc.*, 1968, **115**, 1094.
- T. Maruyama and T. Nakai, *Appl. Phys. Lett.*, 1991, **58**, 2079.
- K. Sawada, M. Ishida, T. Nakamura, and N. Ohtake, *Appl. Phys. Lett.*, 1988, **52**, 1673.
- J. Von Hoene, R. G. Charles, and W. M. Hickam, *J. Phys. Chem.*, 1958, **62**, 1098.

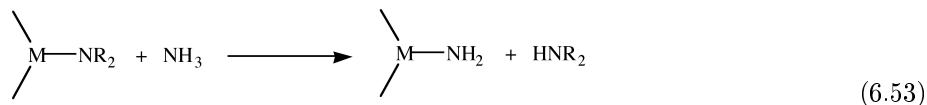
6.5 Nitride Chemical Vapor Deposition

6.5.1 Introduction to Nitride Chemical Vapor Deposition⁷

The refractory nature and high dielectric properties of many nitrides make them attractive for chemical and electronic passivation. As a consequence silicon nitride has become the standard within the semiconductor industry, as both an encapsulation layer and as an etch mask.

In a similar manner to oxide growth by chemical vapor deposition (CVD), two sources are generally required for binary nitride CVD: the element of choice and a nitrogen source. However, unlike the CVD of oxides, elemental nitrogen (N_2) is not reactive, even at elevated temperatures, thereby requiring plasma enhancement. Even with plasma enhanced CVD (PECVD), N_2 does not yield high quality films. As a substitute for N_2 , ammonia (NH_3) has found general acceptance as a suitable nitrogen source. It is a gas, readily purified and cheap, however, it is of low reactivity at low temperatures. PECVD has therefore found favor for low temperature NH_3 -based precursor systems.

Recent attempts to lower deposition temperatures have included the use of more reactive sources (e.g., H_2NNH_2) and precursors containing nitrogen as a coordinated ligand. Probably the most important discovery with respect to nitride deposition is the use of a transamination reaction between amido compounds and ammonia ((6.53)).



6.5.1.1 Bibliography

- D. M. Hoffman, *Polyhedron*, 1994, **13**, 1169.

6.5.2 Chemical Vapor Deposition of Silicon Nitride and Oxynitride⁸

6.5.2.1 Introduction

Stoichiometric silicon nitride (Si_3N_4) is used for chemical passivation and encapsulation of silicon bipolar and metal oxide semiconductor (MOS) devices, because of its extremely good barrier properties for water and sodium ion diffusion. Water causes device metallization to corrode, and sodium causes devices to become electrically unstable. Silicon nitride is also used as a mask for the selective oxidation of silicon, and as a strong dielectric in MNOS (metal-nitride-oxide-silicon) structures.

The use of ion implantation for the formation of active layers in GaAs MESFET devices (Figure 6.17) allow for control of the active layer thickness and doping density. Since implantation causes structural disorder, the crystal lattice of the GaAs must be subjected to a post implantation rapid thermal anneal step to repair the damage and to activate the implanted species. The required annealing temperature (> 800 °C) is higher than the temperature at which GaAs decomposes. Silicon nitride encapsulation is used to prevent such dissociation. Silicon nitride is also used for the final encapsulation of GaAs MESFET devices (Figure 6.17).

⁷This content is available online at <http://cnx.org/content/m26117/1.1/>.

⁸This content is available online at <http://cnx.org/content/m26120/1.1/>.

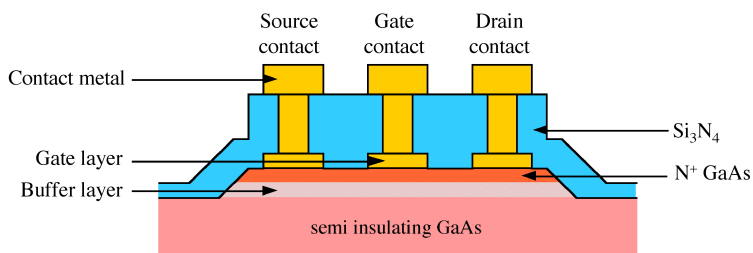


Figure 6.17: Schematic diagrams of a GaAs metal-semiconductor field effect transistor (MESFET). Adapted from A. R. Barron, in *CVD of Nonmetals*, Ed. W. S. Rees, Jr., Wiley, NY (1996).

The deposition of Si_3N_4 is a broadly practiced industrial process using either grown by low pressure CVD (LPCVD) or plasma enhanced CVD (PECVD) with comparable properties for the grown films (Table 6.9).

Deposition	LPCVD	PECVD
Growth temperature ($^{\circ}\text{C}$)	700 - 800	250 - 350
Composition	$\text{Si}_3\text{N}_4(\text{H})$	SiN_xH_y
Si/N ratio	0.75	0.8 - 1.2
Atom% H	4 - 8	20 - 25
Dielectric constant	6 - 7	6 - 9
Refractive index	2.01	1.8 - 2.5
Resistivity ($\Omega\cdot\text{cm}$)	1016	106 - 1015
Band gap (eV)	5	4 - 5

Table 6.9: Summary of the properties of silicon nitride grown in typical commercial systems.

One of the disadvantages of Si_3N_4 is its high dielectric constant that may limit device speed at higher operating frequencies. It is hoped that silicon oxynitride (SiON) films will exhibit the best properties of Si_3N_4 and SiO_2 , namely the passivation and mechanical properties of Si_3N_4 and the low dielectric constant and low stress of SiO_2 .

A summary of some typical CVD systems for silicon nitride is given in Table 6.10.

Silicon precursor	Nitrogen source	Carrier gas	CVD method	Deposition temp. ($^{\circ}\text{C}$)	Comment
<i>continued on next page</i>					

SiH ₄	NH ₃	N ₂	APCVD	70 - 900	
SiH ₄	NH ₃	Ar/N ₂	PECVD	20 - 600	Commercial process
SiH ₄	N ₂	N ₂	PECVD	70 - 300	Porous films
SiCl ₂ H ₂	NH ₃	N ₂	LPCVD	700 - 900	Commercial process
Si ₂ Cl ₆	NH ₃	-	LPCVD	450 - 850	
Et ₂ SiH ₂	NH ₃	-	LPCVD	650 - 725	C impurities
RSi(N ₃) ₃ (R = Et, ^t Bu)	-	-	LPCVD	450 - 600	Danger – precursor explosive
MeSiH(NH) _n	-	NH ₃ /H ₂	APCVD	600 - 800	Significant C content
Si(NMe ₂) _{4-n} H _n	-	He	APCVD	600 - 750	Significant C content
Si(NMe ₂) _{4-n} H _n	NH ₃	He	APCVD	600 - 750	No C contamination

Table 6.10: Precursors and deposition conditions for Si₃N₄ CVD.

6.5.2.2 CVD of silicon nitride from hydrides and chlorides

The first commercial growth of silicon nitride was by the reaction of SiH₄ and NH₃ by either atmospheric pressure CVD (APCVD) or PECVD. Film growth using APCVD is slower and requires higher temperatures and so it has been generally supplanted by plasma growth, however, film quality for APCVD is higher due to the lower hydrogen content. While thermally grown films are close to stoichiometric, PECVD films have a composition in which the S/N ratio is observed to vary from 0.7 - 1.1. The non-stoichiometric nature of PECVD films is explained by the incorporation of significant hydrogen in the films (10 - 30%). PECVD of SiN_x using SiH₄/N₂ leads to electronically leaky films due to the porous nature of the films, however, if an electron cyclotron resonance (ECR) plasma is employed, SiN_x films of high quality may be deposited on ambient temperature substrates.

The more recent commercial methods for silicon nitride deposition involves LPCVD using SiCl₂H₂ as the silicon source in combination with NH₃ at 700 - 900 °C. The reduced pressure of LPCVD has the advantages of high purity, low hydrogen content, stoichiometric films, with a high degree of uniformity, and a high wafer throughput. It is for these reasons that LPCVD is now the method of choice in commercial systems. A large excess of NH₃ is therefore used in commercial systems to obtain stoichiometric films. Silicon nitride has also been prepared from SiCl₄/NH₄, SiBr₄/NH₃, and, more recently, Si₂Cl₆/NH₃.

Silicon oxynitride (SiON) may be prepared by the use of any of the precursors used for silicon nitride with the addition of either N₂O or NO as an oxygen source. The composition and properties of the SiO_xN_y films may be varied from SiO₂-like to Si₃N₄-like by the variation of the reactant flow rates.

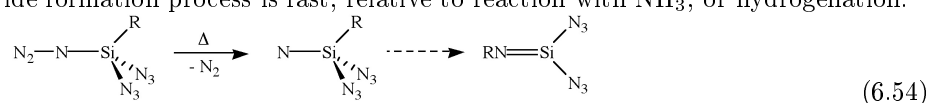
SiCl₂H₂ gas plumbing to a LPCVD reactor must be thermally insulated to prevent condensation that would otherwise lead to hazy deposits on the film. The volatile by-products from CVD produce NH₄Cl at the exhaust of the reaction tube, and in the plumbing and pumping system. It would be desirable, therefore, to find an alternative, chlorine-free silicon source with none of the toxicity or pyrophoricity problems associated with SiH₄. It is for this reason that organosilicon compounds have been investigated.

6.5.2.3 CVD from organosilicon precursors

Diethylsilane, Et_2SiH_2 , has shown promise as a replacement for SiH_4 in the low temperature LPCVD of SiO_2 , and has been investigated as a source for SiN_x and SiO_xN_y films. Deposition by LPCVD in the presence of NH_3 produces SiN_x films, in which the carbon contamination (4 - 9%) depends on the partial pressure of the Et_2SiH_2 . The presence of carbon raises the refractive index (2.025 - 2.28) with respect to traditional LPCVD films (2.01). Mixtures of Et_2SiH_2 , NH_3 , and N_2O deposit SiO_xN_y films where the composition is controlled by the $\text{NH}_3:\text{N}_2\text{O}$ ratio.

6.5.2.3.1 CVD from silicon-nitrogen compounds

The incorporation of carbon into silicon nitride films is a persistent problem of organosilicon precursors. Several studies have been aimed at developing single source precursors containing a Si-N bond rather than Si-C bonds. Polyazidosilanes, $\text{R}_n\text{Si}(\text{N}_3)_{4-n}$, are low in carbon and hydrogen, reasonably volatile, and contain highly activated nitrogen, however, they represent a significant explosive hazard: *they are explosive with an equivalent force to TNT*. Films deposited using $\text{EtSi}(\text{N}_3)_3$ and $(\text{tBu})\text{Si}(\text{N}_3)_3$ showed promise, despite the observation of oxygen and carbon. Pyrolytic studies on the azide precursors suggest that the primary decomposition step is the loss of dinitrogen, which is followed by migration of the alkyl onto the remaining nitrogen, (6.54). The fact that neither the addition of NH_3 or H_2 influence the film deposition rate suggest that the intramolecular nitride formation process is fast, relative to reaction with NH_3 , or hydrogenation.



Carbon incorporation is also observed for the APCVD deposition from $\text{Si}(\text{NMe}_2)_n\text{H}_{4-n}$ ($n = 2 - 4$). However, using the Hoffman transamination reaction, deposition in the presence of NH_3 completely removed carbon incorporation into the stoichiometric Si_3N_4 film. From FTIR data, the hydrogen content was estimated to be 8 - 10 atom percent. While the $\text{Si}(\text{NMe}_2)_n\text{H}_{4-n}/\text{NH}_3$ system does not provide substantially lower temperatures than APCVD using SiH_4/NH_3 growth rates are significantly higher. Unlike the azide precursors, $\text{Si}(\text{NMe}_2)_n\text{H}_{4-n}$ are easier to handle than either SiH_4 or SiCl_2H_2 .

6.5.2.4 Bibliography

- J. C. Barbour, H. J. Stein, O. A. Popov, M. Yoder, and C.A. Outten, *J. Vac. Sci. Technol. A.*, 1991, **9**, 480.
- J. A. Higgins, R. L. Kuvas, F. H. Eisen, and D. R. Chen, *IEEE Trans. Electron. Devices*, 1978, **25**, 587.
- D. M. Hoffman, *Polyhedron*, 1994, **13**, 1169.
- W. Kellner, H. Kniepkamp, D. Repow, M. Heinzl, and H. Boroleka, *Solid State Electron.*, 1977, **20**, 459.
- T. Makino, *J. Electrochem. Soc.*, 1983, **130**, 450.
- C. T. Naber and G. C. Lockwood, in *Semiconductor Silicon*, Eds. H. R. Huff and R. R. Burgess. The Electrochemical Society, Softbound Proceedings Series, Princeton, NJ (1973).
- J. E. Schoenholtz, D. W. Hess, *Thin Solid Films*, 1987, **148**, 285.

6.5.3 Chemical Vapor Deposition of Aluminum Nitride⁹

6.5.3.1 Introduction

Aluminum nitride (AlN) has potential for significant applications in microelectronic and optical devices. It has a large direct bandgap ($E_{g,\text{dir}} = 6.28$ eV), extremely high melting point (3000 °C), high thermal

⁹This content is available online at <<http://cnx.org/content/m26132/1.1/>>.

conductivity (2.6 W/cm.K), and a large dielectric constant ($\epsilon = 9.14$). In present commercial microelectronic devices, AlN is used most often as a packaging material, allowing for the construction of complex packages with many signal, ground, power, bonding, and sealing layers. Aluminum nitride is especially useful for high power applications due to its enhanced thermal conductivity. Chemical vapor deposition (CVD) grown thin films of AlN have been centered upon its use as a high gate-insulation layer for MIS devices, and a dielectric in high-performance capacitors. One additional property of AlN that makes it a promising insulating material for both Si and GaAs devices is that its thermal expansion coefficient is almost identical to both of these semiconductors.

The lack of a suitably volatile homoleptic hydride for aluminum (AlH_3 is an involatile polymeric species) led to the application of aluminum halides and organometallic compounds as precursors. A summary of selected precursor combinations is given in Table 6.11.

Aluminum precursor	Nitrogen source	Carrier gas	CVD method	Deposition temp. ($^{\circ}\text{C}$)	Comments
$\text{AlCl}_3(\text{NH}_3)$	-	N_2	LPCVD	700 - 1400	NH_4Cl present
AlBr_3	NH_3	N_2	APCVD	400 - 900	Br present
AlBr_3	N_2	N_2	LPCVD	520 - 560	oriented growth
AlMe_3	NH_3	H_2	LPCVD	1200	
AlMe_3	NH_3	He	APCVD	350 - 400	
AlMe_3	pre-cracked NH_3	H_2/He	APCVD	310 - 460	N-H and Al-N bonds detected
AlMe_3	$^t\text{BuNH}_2$ or $^i\text{PrNH}_2$	H_2	APCVD	400 - 600	high C content, low N
AlMe_3	Me_3SiN_3	H_2	APCVD	300 - 450	very high C content
$[\text{R}_2\text{Al}(\text{NH}_2)]_3$ (R = Me, Et)		H_2	LPCVD	400 - 800	poor film quality, high C content
$[\text{R}_2\text{AlN}_3]_3$ (R = Me, Et)		-	LPCVD	400 - 500	unreacted precursor present on film
$\text{Al}(\text{NMe}_2)_3$	NH_3	He	APCVD	100 - 500	amorphous 100 - 200 $^{\circ}\text{C}$, crystalline 300 - 500 $^{\circ}\text{C}$

Table 6.11: Precursors and deposition conditions for AlN CVD.

6.5.3.2 CVD from halides

The observation that AlN powder may be produced upon the thermal decomposition of the $\text{AlCl}_3(\text{NH}_3)$ complex, prompted initial studies on the use of $\text{AlCl}_3/\text{NH}_3$ for the CVD of AlN films. Initially, the low volatility of AlCl_3 (a polymeric chain structure) required that the $\text{AlCl}_3(\text{NH}_3)$ complex to be used as a single precursor. Low pressure CVD (LPCVD) at 5 -10 Torr resulted in deposition of AlN films, although

films deposited below 1000 °C were contaminated with NH₄Cl, and all the films contained chlorine. Films with reasonable electrical properties were prepared by the use of the more volatile *tris*-ammonia complex, AlCl₃(NH₃)₃. The dielectric constant for films grown at 800 - 1000 °C (11.5) is higher than bulk AlN (9.14) and also than that of the films grown at 1100 °C (8.1). All the films were polycrystalline with the grain size increasing with increasing deposition temperatures and preferred orientation was observed only for the films grown below 1000 °C.

Aluminum bromide is a dimeric volatile compound, [Br₂Al(μ-Br)]₂, and is more attractive as a CVD source, than AlCl₃. Deposition of AlN films can be accomplished using AlBr₃ and NH₃ in an APCVD system with H₂ as the carrier gas. The mechanism of film growth has been proposed (Figure 6.18).

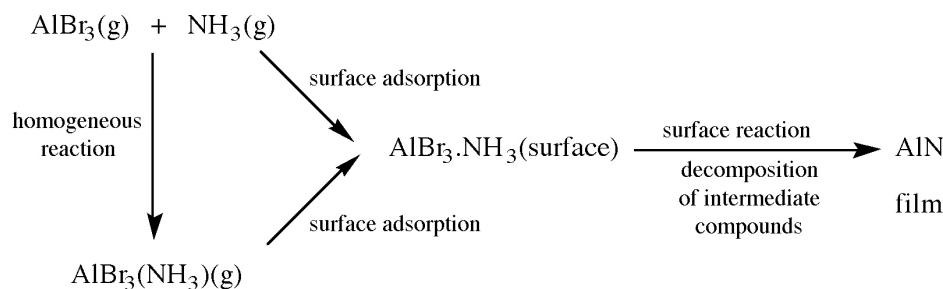


Figure 6.18: Mechanism of APCVD film growth of AlN using AlBr₃ and NH₃.

Due to the high temperatures required (750 °C) for good quality AlN film growth from AlBr₃, PECVD was investigated. Using an AlBr₃-H₂-N₂ gas mixture and a 2450 MHz microwave (100 - 1000 W) plasma source, AlN films were grown. The maximum deposition rate occurred with an N₂/AlBr₃ ratio of ca. 20 and a substrate temperature ca. 600 °C.

6.5.3.3 CVD from aluminum alkyls

Based upon the successful metal organic CVD (MOCVD) growth of AlGaAs using the alkyl derivatives, AlR₃, it was logical to extend MOCVD to aluminum nitride. Initial studies were performed using AlMe₃ and NH₃ with H₂ carrier gas. While these films are generally of high quality, the temperature of deposition is incompatible with semiconductor processing (being above both the melting point of most metallization alloys and the temperature at which dopant migration becomes deleterious). Lower temperatures (as low as 350 °C) were explored, however significant pre-reaction was observed between AlMe₃ and NH₃; causing depletion of the reactants in the deposition zone, reducing the growth rate and leading to non-uniform deposits. Two routes have been investigated by which this problem can be circumvented.

PECVD successfully lowers the deposition temperature, although, degradation of the substrate surface by ion bombardment is a significant drawback. Given that it is the ammonia decomposition that represents the highest energy process, pre-cracking should lower the overall deposition temperature. This is indeed observed for the AlMe₃/NH₃-based AlN system where growth is achieved as low as 584 °C if the NH₃ is catalytically cracked over a heated tungsten filament (1747 °C). In fact, with catalytic pre-cracking, deposition rates were observed to be an order of magnitude greater than for PECVD at the same temperatures, resulting in films that were crystalline with columnar growth. For this approach to low-temperature MOCVD growth of AlN the only major drawback is the presence of residual N-H and AlN-N groups detected by FT-IR.

Chemical solutions to the high stability of NH₃ have primarily centered upon the use of alternative nitrogen sources. The use of the volatile nitrogen source hydrazine (N₂H₄), has allowed for the growth

of AlN at temperatures as low as 220 °C, however, hydrazine is extremely toxic and highly unstable, restricting its commercial application. Primary amines, such as ^tBuNH₂ or ⁱPrNH₂, allow for deposition at modest temperatures (400 - 600 °C). The high carbon incorporation, as high as 17% precludes their adoption. A similar problem is observed with the use of trimethylsilylazide, Me₃SiN₃. The presence of carbon contamination in the deposition of Al films and AlGaAs epitaxial layers has been attributed to the use of AlMe₃. Therefore attempts have been made to use alternative aluminum precursors.

Interest in the mechanism of nucleation and atomic layer growth of AlN has prompted several mechanistic studies of the formation of Al-N bonds on the growth surface. All the studies concurred that the mechanism involves a step-wise reaction where the amide (-NH₂-) groups form covalent bonds to aluminum irrespective of substrate. A schematic representation of the process is shown in Figure 6.19.

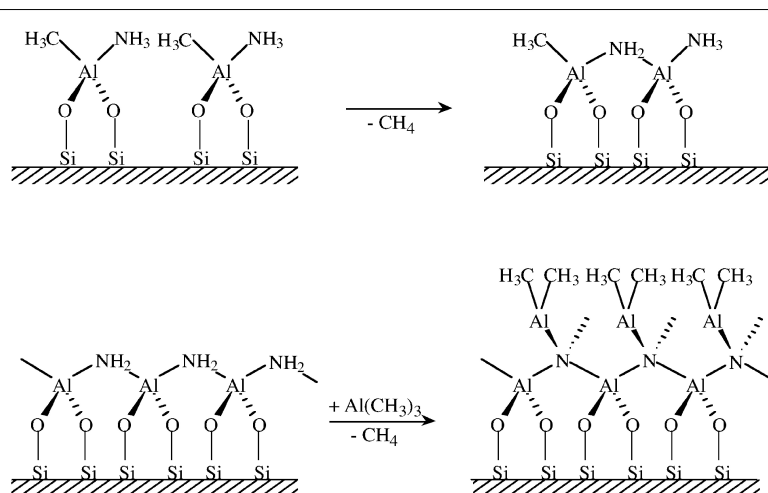
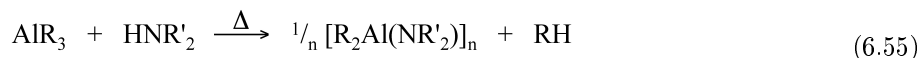


Figure 6.19: A schematic representation of the proposed step-wise reaction involving the formation of amide (-NH₂-) groups covalently bound to aluminum during the MOCVD growth of AlN using AlMe₃/NH₃. (Adapted from M. E. Bartram, T. A. Michalske, J. W. Rogers, Jr., and R. T. Paine, *Chem. Mater.*, 1993, **5**, 1424).

6.5.3.4 CVD from aluminum amide and related compounds

The reaction between aluminum alkyls and amines ((6.55)), as well as the formation of AlN powders from the pyrolysis of AlMe₃(NH₃) ((6.56)), lead to the misguided concept that the route to high-purity AlN would be through the so-called single source precursor route.



The trimeric dimethylaluminum amide, [Me₂Al(NH₂)]₃ (Figure 6.20a), was originally used as a single source precursor for growth of AlN under LPCVD conditions using a hot walled reactor, although subsequent deposition was also demonstrated in a cold walled system. Film quality was never demonstrated for electronic applications, but the films showed promise as fiber coatings for composites. The concept of using a trimeric

single source precursor for AlN was derived from the observation of Al_3N_3 cycles as the smallest structural fragment in wurtzite AlN. However, detailed mechanistic studies indicate that under gas phase thermolysis the trimeric precursor $[\text{Me}_2\text{Al}(\text{NH}_2)]_3$ is in equilibrium with (or decomposes to) dimeric (Figure 6.20b) and monomeric (Figure 6.20c) compounds. Furthermore, nitrogen-poor species (Figure 6.20d) were also observed by TOF-mass spectrometry.

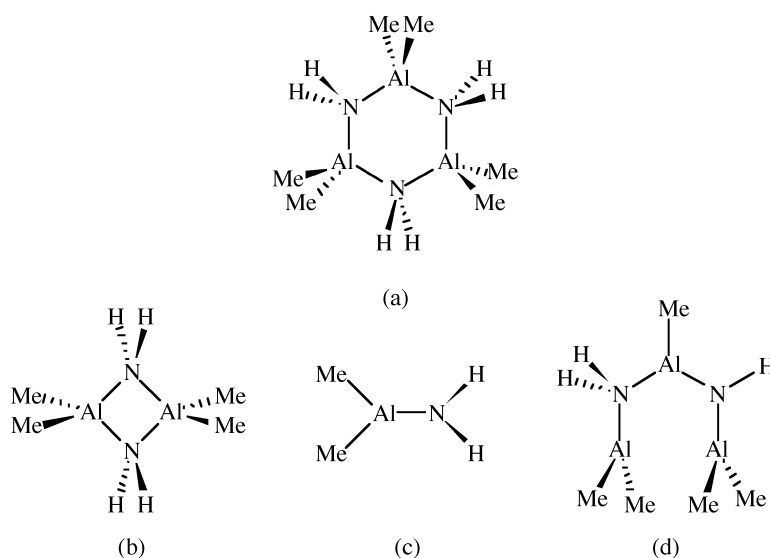


Figure 6.20: The trimeric dimethylaluminum amide (a) used as a single source precursor for growth of AlN, and the decomposition products (b - d) observed by TOF-mass spectrometry.

Following the early reports of single source precursor routes, a wide range of compounds have been investigated, including $[\text{Al}(\text{NR}_2)_3]_2$, $[\text{HAl}(\text{NR}_2)_2]_2$ ($\text{R} = \text{Me}, \text{Et}$), and $[\text{Me}_2\text{AlN}(\text{iPr})_2]_2$, all of which gave AlN, but none of these precursors give films of superior quality comparable to that obtained from traditional CVD. In particular, the films contained significant carbon contamination, prompting further investigations into the efficacy of, N-C bond free, dialkylaluminum azides, $[\text{R}_2\text{Al}(\text{N}_3)]_3$, as LPCVD precursors.

While aluminum *tris*-amides, $\text{Al}(\text{NR}_2)_3$ were shown to give carbon-contaminated films, APCVD carried-out with NH_3 as the carrier gas results in carbon-free AlN film growth as low as 100 °C. The reason for the deposition of high quality films at such low temperatures resides with the Hoffman transamination reaction between the primary amido unit and ammonia. The crystallinity, bandgap and refractive index for the AlN grown by APCVD using $[\text{Al}(\text{NMe}_2)_3]_2$ and NH_3 are dependent on the deposition temperature. Films grown at 100 - 200 °C are amorphous and have a low bandgap and low refractive index. Above 300 °C, the films are crystalline, and have a refractive index close to that of bulk AlN (1.99 - 2.02), with a bandgap (≤ 5.77 eV) approaching the values reported for polycrystalline AlN (5.8 - 5.9 eV).

6.5.3.5 Bibliography

- J. L. Dupuie and E. Gulari, *J. Vac. Sci. Technol. A*, 1992, **10**, 18.
- D. M. Hoffman, *Polyhedron*, 1994, **13**, 1169.
- L. V. Interrante, W. Lee, M. McConnell, N. Lewis, and E. Hall, *J. Electrochem. Soc.*, 1989, **136**, 472.
- H. M. Manasevit, F. M. Erdmann, and W. I. Simpson, *J. Electrochem. Soc.*, 1971, **118**, 1864.

- Y. Pauleau, A. Bouteville, J.J. Hantzpergue, J. C Remy, and A. Cachard, *J. Electrochem. Soc.*, 1980, **127**, 1532.
- Y. Someno, M. Sasaki, and T. Hirai, *Jpn. J. Appl. Phys.*, 1990, **29**, L358.

6.6 Metal Organic Chemical Vapor Deposition of Calcium Fluoride¹⁰

The chemical vapor deposition (CVD) of metal fluorides has been much less studied than that of oxides, pnictides, or chalcogenides. As may be expected where a volatile fluoride precursor is available then suitable films may be grown. For example, Group 5 (V, Nb, Ta), 6 (Mo, W), and 7 (Re) transition metals are readily deposited from fluoride-hydrogen mixtures. While the use of fluorine is discouraged on safety grounds, many of the fluorinated alkoxide or β -diketonate ligands employed for metal oxide metal organic chemical vapor deposition (MOCVD) are predisposed to depositing metal fluorides. The use of fluorine substituted derivatives is because they are often more volatile than their hydrocarbon analogs, and therefore readily used for both atmospheric and low pressure CVD. To minimize the unwanted formation of metal fluorides, water vapor is incorporated in the gas stream, and it is common to perform post-deposition hydrolytic anneals. However, there exist a number of applications where fluorides are required. For example, the highly insulating nature of CaF_2 and SrF_2 has prompted investigations into their use as a gate insulator in GaAs-based metal insulator semiconductor field effect transistor (MISFET) devices. It should be noted that while CaF_2 is a good insulator, the CaF_2/GaAs interface has a high interface trap density, requiring a passivation buffer layer to be deposited on GaAs prior to CaF_2 growth.

One of the difficulties with the use of CaF_2 (and SrF_2) on GaAs is the lattice mismatch (Table 6.12), but this may be minimized by the use of solid solutions between CaF_2 - SrF_2 . The composition $\text{Ca}_{0.44}\text{Sr}_{0.56}\text{F}_2$ is almost perfectly lattice-matched to GaAs. Unfortunately, the thermal expansion coefficient differences between GaAs and CaF_2 - SrF_2 produce strains at the film/substrate interface under high temperature growth conditions. The solution to this latter problem lies in the low temperature deposition of CaF_2 - SrF_2 by CVD.

Compound	Lattice constant (Å)
CaF_2	5.46
SrF_2	5.86
BaF_2	6.20
GaAs	5.6532

Table 6.12: Lattice parameters of Group 2 (II) fluorides in comparison with GaAs.

Polycrystalline CaF_2 may be grown by the pyrolytic decomposition of $\text{Ca}(\text{C}_5\text{Me}_5)_2$ (Figure 6.21a) in either SiF_4 or NF_3 . Deposition at 150 °C results in polycrystalline films with high levels of carbon (18%) and oxygen (7%) impurities limiting the films usefulness in electronic applications. However, significantly higher purity films may be grown at 100 °C using the photo-assisted decomposition of $\text{Ca}(\text{hfac})_2$ (Figure 6.21b). These films were deposited at 30 Å/min and showed a high degree of crystallographic preferred orientation.

¹⁰This content is available online at <<http://cnx.org/content/m26116/1.3/>>.

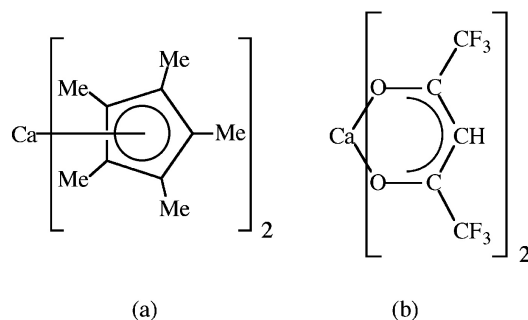


Figure 6.21: CaF_2 MOCVD precursors.

The mechanism enabling fluoride transfer to the metal (from the carbon of fluorinated alkoxide ligands) has been investigated. MOCVD employing $[\text{Na}(\text{OR}_f)]_4$ and $\text{Zr}(\text{OR}_f)_4$ [$\text{OR}_f = \text{OCH}(\text{CF}_3)_2$ and $\text{OCMe}_{3-n}(\text{CF}_3)_n$, $n = 1 - 3$] gives NaF and ZrF_4 films, respectively, with volatile fluorocarbon side-products. Analysis of the organic side-products indicated that decomposition occurs by transfer of fluorine to the metal in conjunction with a 1,2-migration of a residual group on the alkoxide, to form a ketone (Figure 6.22). The migration is increasingly facile in the order $\text{CF}_3 \ll \text{CH}_3 \leq \text{H}$. The initial M-F bond formation has been proposed to be as a consequence of the close $\text{M} \cdots \text{F}$ agostic interactions observed for some fluoroalkoxide and fluoro- β -diketonates.

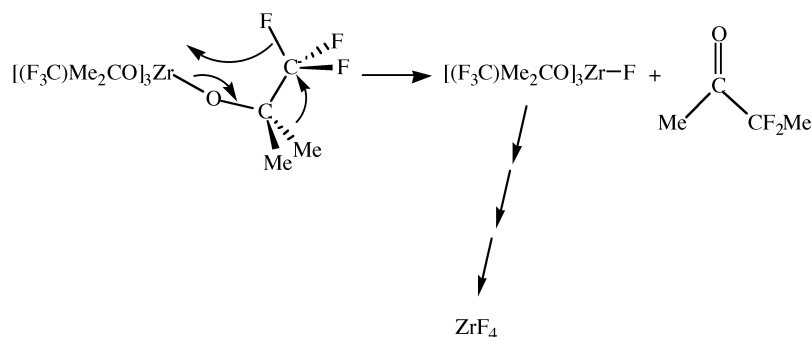


Figure 6.22: Proposed mechanism for the decomposition of fluorinated alkoxide compounds. (Adapted from J. A. Samuels, W. -C. Chiang, C. -P. Yu, E. Apen, D. C. Smith, D. V. Baxter, K. G. Caulton, *Chem. Mater.*, 1994, **6**, 1684).

6.6.1 Bibliography

- A. R. Barron, in *CVD of Nonmetals*, W. S. Rees, Jr. (ed), Wiley, New York (1996).

- B. D. Fahlman and A. R. Barron, *Adv. Mater. Opt. Electron.*, 2000, **10**, 223.
- H. Heral. L. Bernard, A. Rocher, C. Fontaine, A. Munoz-Jague, *J. Appl. Phys.*, 1987, **61**, 2410.
- J. A. Samuels, W. -C. Chiang, C. -P. Yu, E. Apen, D. C. Smith, D. V. Baxter, K. G. Caulton, *Chem. Mater.*, 1994, **6**, 1684.
- W. Vere, K. J. Mackey, D. C. Rodway, P. C. Smith, D. M Frigo, D. C. Bradley, *Angew. Chem. Int. Ed. Engl. Adv. Mater.*, 1989, **28**, 1581.

6.7 Precursors for Chemical Vapor Deposition of Copper¹¹

NOTE: This module was developed as part of the Rice University course CHEM-496: *Chemistry of Electronic Materials*. This module was prepared with the assistance of Wei Zhao.

6.7.1 Introduction

Chemical vapor deposition (CVD) is a process for depositing solid elements and compounds by reactions of gas-phase molecular precursors. Deposition of a majority of the solid elements and a large and ever-growing number of compounds is possible by CVD.

Most metallization for microelectronics today is performed by the physical vapor deposition (PVD) processes of evaporation and sputtering, which are often conceptually and experimentally more straightforward than CVD. However, the increasing importance of CVD is due to a large degree to the advantages that it holds over physical vapor deposition. Foremost among these are the advantages of conformal coverage and selectivity. Sputtering and evaporation are by their nature line-of-sight deposition processes in which the substrate to be coated must be placed directly in front of the PVD source. In contrast, CVD allows any substrate to be coated that is in a region of sufficient precursor partial pressure. This allows the uniform coating of several substrate wafers at once, of both sides of a substrate wafer, or of a substrate of large size and/or complex shape. The PVD techniques clearly will also deposit metal on any surface that is in line of sight. On the other hand, it is possible to deposit selectively on some substrate materials in the presence of others using CVD, because the deposition is controlled by the surface chemistry of the precursor/substrate pair. Thus, it may be possible, for example, to synthesize a CVD precursor that under certain conditions will deposit on metals but not on an insulating material such as SiO₂, and to exploit this selectivity, for example, in the fabrication of a very large-scale integrated (VLSI) circuit. It should also be pointed out that, unlike some PVD applications, CVD does not cause radiation damage of the substrate.

Since the 1960s, there has been considerable interest in the application of metal CVD for thin-film deposition for metallization of integrated circuits. Research on the thermal CVD of copper is motivated by the fact that copper has physical properties that may make it superior to either tungsten or aluminum in certain microelectronics applications. The resistivity of copper (1.67 mW.cm) is much lower than that of tungsten (5.6 mW.cm) and significantly lower than that of aluminum (2.7 mW.cm). This immediately suggests that copper could be a superior material for making metal interconnects, especially in devices where relatively long interconnects are required. The electromigration resistance of copper is higher than that of aluminum by four orders of magnitude. Copper has increased resistance to stress-induced voidage due to its higher melting point versus aluminum. There are also reported advantages for copper related device performance such as greater speed and reduced cross talk and smaller RC time constants. On the whole, the combination of superior resistivity and intermediate reliability properties makes copper a promising material for many applications, provide that suitable CVD processes can be devised.

6.7.1.1 Applications of metal CVD

There are a number of potential microelectronic applications for metal CVD, including gate metallization (deposit on semiconductor), contact metallization (deposit on semiconductor), diffusion barrier metallization

¹¹This content is available online at <<http://cnx.org/content/m25428/1.4/>>.

(deposit on semiconductor), interconnect metallization (deposit on insulator and conductor or semiconductor). Most of the relevant features of metal CVD are found in the interconnect and via fill applications, which we briefly describe here. There are basically two types of metal CVD processes that may occur:

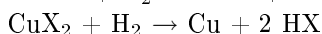
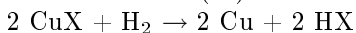
- (1) Blanket or nonselective deposition, in which deposition proceeds uniformly over a variety of surfaces.
- (2) Selective deposition in which deposition only occurs on certain types of surfaces (usually semiconductors or conductors, but not insulators).

A primary application of blanket metal CVD is for interconnects. The conformal nature of the CVD process is one of the key advantages of CVD over PVD and is a driving force for its research and development. The degree of conformality is usually described as the “step coverage”, which is normally defined as the ratio of the deposit thickness on the step sidewall to the deposit thickness on the top surface. Another application for blanket metal CVD is via hole filling to planarize each level for subsequent processing. This is achieved by depositing a conformal film and etching back to the insulator surface, leaving the metal “plug” intact. Another unique aspect of CVD is its potential to deposit films selectively, which would eliminate several processing steps required to perform the same task. The primary application for selective metal CVD would be for via hole filling. Ideally, deposition only occurs on exposed conductor or semiconductor surfaces, so filling of the via hole is achieved in a single step.

6.7.2 Copper CVD

The chemical vapor deposition of copper originally suffered from a lack of readily available copper compounds with the requisite properties to serve as CVD precursors. The successful development of a technologically useful copper CVD process requires first and foremost the design and synthesis of a copper precursor which is volatile, i.e., possesses an appreciable vapor pressure and vaporization rate to allow ease in transportation to the reaction zone and deposition at high growth rates. Its decomposition mechanism(s) should preferably be straightforward and lead to the formation of pure copper and volatile by-products that are nonreactive and can be cleanly removed from the reaction zone to prevent film, substrate, and reactor contamination. Gaseous or liquid sources are preferred to solid sources to avoid undesirable variations in vaporization rates because of surface-area changes during evaporation of solid sources and to permit high levels of reproducibility and control in source delivery. Other desirable features in precursor selection include chemical and thermal stability to allow extended shelf life and ease in transport and handling, relative safety to minimize the industrial and environmental impact of processing and disposal, and low synthesis and production costs to ensure an economically viable process.

Several classes of inorganic and metalorganic sources have been explored as copper sources. Inorganic precursors for copper CVD used hydrogen reduction of copper halide sources of the type CuX or CuX_2 , where X is chlorine (Cl) or fluorine (F):



The volatility of copper halides is low, the reactions involved require prohibitively high temperatures (400 - 1200 °C), lead to the production of corrosive by-products such as hydrochloric and hydrofluoric acids (HCl and HF), and produce deposits with large concentrations of halide contaminants. Meanwhile, the exploration of metalorganic chemistries has involved various copper(II) and copper(I) source precursors, with significant advantages over inorganic precursors.

6.7.3 From Cu(II) precursors

6.7.3.1 Volatile Cu(II) compounds

Copper was known to form very few stable, volatile alkyl or carbonyl compounds. This was thought to eliminate the two major classes of compounds used in most existing processes for CVD of metals or compound semiconductors. Copper halides have been used for chemical vapor transport growth of Cu-containing semiconductor crystals. But the evaporation temperatures needed for copper halides are much higher than those

needed for metal-organic compounds. Film purity and resistivity were also a problem, possibly reflecting the high reactivity of Si substrates with metal halides.

Cu(II) compounds that have been studied as CVD precursors are listed in Table 6.13. The structural formulas of these compounds are shown in Figure 6.23 along with the ligand abbreviations in Table 6.14. Each compound contains a central Cu(II) atom bonded to two singly charged β -diketonate or β -ketoiminate ligands. Most of them are stable, easy to synthesize, transport and handle.

Compound	Evaporation temp. ($^{\circ}\text{C}$)	Deposition temp. ($^{\circ}\text{C}$)	Carrier gas	Reactor pressure (Torr)
$\text{Cu}(\text{acac})_2$	180 - 200	225 - 250	H_2/Ar	760
$\text{Cu}(\text{hfac})_2$	80 - 95	250 - 300	H_2	760
$\text{Cu}(\text{tfac})_2$	135 - 160	250 - 300	H_2	760
$\text{Cu}(\text{dpm})_2$	100	400	none	$<10^{-2}$
$\text{Cu}(\text{ppm})_2$	100	400	none	<0.3
$\text{Cu}(\text{fod})_2$	-	300 - 400	H_2	10^{-3} - 760
$\text{Cu}(\text{acim})_2$	287	400	H_2	730
$\text{Cu}(\text{nona-F})_2$	85 - 105	270 - 350	H_2	10 - 70
$\text{Cu}(\text{acen})_2$	204	450	H_2	730

Table 6.13: Studies of Cu CVD using Cu(II) compound. Adapted from T. Kodas and M. Hampden-Smith, *The Chemistry of Metal CVD*, VCH Publishers Inc., New York, NY (1994).

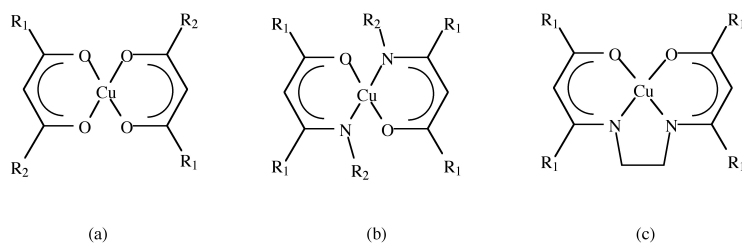


Figure 6.23: Structures of Cu(II) compounds studied as CVD precursors.

Ligand abbreviation	R ₁	R ₂	Structural type
acac	CH ₃	CH ₃	a
hfac	CF ₃	CF ₃	a
tfac	CH ₃	CF ₃	a
dpm	C(CH ₃) ₃	C(CH ₃) ₃	a
ppm	C(CH ₃) ₃	CF ₂ CF ₃	a
fod	C(CH ₃) ₃	CF ₂ CF ₂ CF ₃	a
acim	CH ₃	H	b
nona-F	CF ₃	CH ₂ CF ₃	b
acen	CH ₃	-	c

Table 6.14: Ligand abbreviations for the structures shown in Figure 6.23.

Attention has focused on Cu(II) β -diketonate [i.e., Cu(tfac)₂, Cu(hfac)₂] and Cu(II) β -ketoiminate [i.e., Cu(acim)₂, Cu(acen)₂]. An important characteristic of Cu(II) compounds as CVD precursors is the use of heavily fluorinated ligand such as Cu(tfac)₂ and Cu(hfac)₂ versus Cu(acac)₂. The main effort of fluorine substitution is a significant increase in the volatility of the complex.

6.7.3.2 Synthesis of Cu(II) precursors

6.7.3.2.1 Cu(hfac)₂·nH₂O (n = 0, 1, 2)

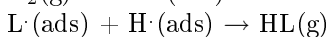
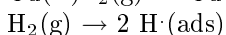
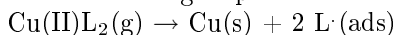
Cu(hfac)₂ is by far the most extensively studied of the Cu(II) CVD precursors. Preparations in aqueous solutions yield the yellow-green dihydrate, Cu(hfac)₂·2H₂O. This is stable in very humid air or at lower temperatures but slowly loses one molecule of water under typical laboratory conditions to form the “grass-green” monohydrate, Cu(hfac)₂·H₂O. The monohydrate, which is commercially available, can be sublimed unchanged and melts at 133 – 136 °C. More vigorous drying over concentrated H₂SO₄ produces the purple anhydrous compound Cu(hfac)₂ (mp = 95 – 98 °C). The purple material is hygroscopic, converting readily into the monohydrate. Other β -diketonate Cu(II) complexes are prepared by the similar method.

6.7.3.2.2 Schiff-base complexes

Schiff-base complexes include Cu(acim)₂, Cu(acen) and Cu(nona-F)₂. The first two of these can be prepared by mixing Cu(NH₃)₄²⁺ (aq) with the pure ligand and by adding freshly prepared solid Cu(OH)₂ to a solution of the ligand in acetone. The synthesis of Cu(nona-F)₂, on the other hand, involved two important developments: the introduction of the silyl enol ether route to the ligand and its conversion in-situ into the desired precursor. The new approach to the ligand was required because, in contrast to non-fluorinated β -diketonates, H(hfac) reacts with amines to produce salts.

6.7.3.3 Reaction mechanism

Starting from the experimental results, a list of possible steps for Cu CVD via H₂ reduction of Cu(II) compounds would include the followings, where removal of adsorbed ligand from the surface is believed to be the rate limiting step:



where L represents any of the singly charged β -diketonate or β -ketoiminate ligands described before. This mechanism gives a clear explanation of the importance of hydrogen being present: in the absence of hydrogen,

HL cannot desorb cleanly into the gas phase and ligand will tend to decompose on the surface, resulting in impurity incorporation into the growing film. The mechanism is also supported by the observation that the deposition reaction is enhanced by the addition of alcohol containing β -hydrogen to the reaction mixture.

More recently, the focus has shifted to Cu(I) compounds including Cu(I) cyclopentadienyls and Cu(I) β -diketonate. The Cu(I) β -diketonate in particular show great promise as Cu CVD precursors and have superseded the Cu(II) β -diketonate as the best family of precursors currently available.

6.7.4 From Cu(I) precursors

6.7.4.1 Precursor design

The Cu(I) compounds that have been investigated are described in Figure 6.24. These species can be broadly divided into two classes, CuX and XCuL_n , where X is a uninegative ligand and L is a neutral Lewis base electron pair donor. The XCuL_n class can be further subdivided according to the nature of X and L.

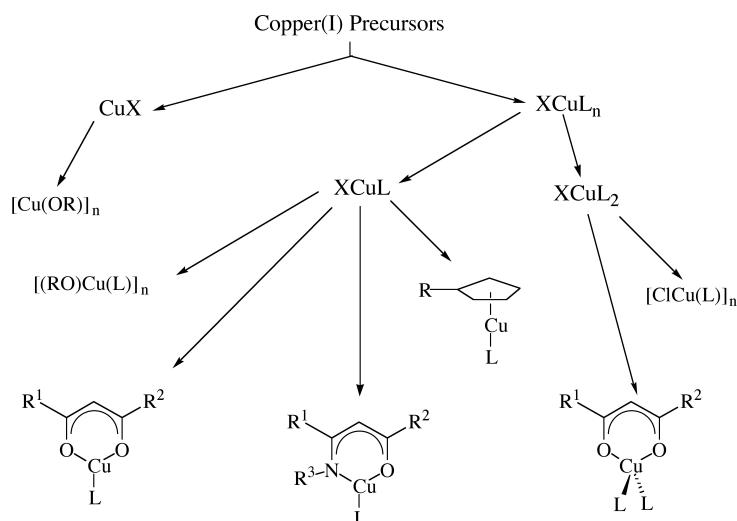


Figure 6.24: Copper(I) precursors used for CVD. Adapted from T. Kodas and M. Hampden-Smith, *The Chemistry of Metal CVD*, VCH Publishers Inc., New York, NY (1994).

Compounds of general formula CuX are likely to be oligomeric resulting in a relatively low vapor pressure. The presence of a neutral donor ligand, L, is likely to reduce the extent of oligomerization compared to CuX by occupying vacant coordination sites. Metal alkoxide compounds are expected to undergo thermal decomposition by cleavage of either M-O or O-C bonds.

Organo-copper(I) compounds, RCuL , where R is alkyl, are thermally unstable, but cyclopentadienyl compounds are likely to be more robust due to the π -bonding of the cyclopentadienyl ligand to the copper center. At the same time, the cyclopentadienyl ligand is sterically demanding, occupies three coordination sites at the metal center, and thereby reduces the desire for oligomerization. In general, a cyclopentadienyl ligand is a poor choice to support CVD precursors, especially with electropositive metals, because this ligand is unlikely to be liable. Compounds in the family XCuL_2 , where X is a halide and L is a triorganophosphine, exhibit relatively high volatility but are thermally stable with respect to formation of copper at low temperatures. These species are therefore suitable as products of etching reactions of copper films.

A number of researchers have demonstrated the potential of a series of β -diketonate Cu(I) compounds, $(\beta\text{-diketonate})\text{CuL}_n$, where L is Lewis base and $n = 1$ or 2 , that fulfill most of the criteria outlined for precursor design before. These species were chosen as copper precursors for the following reasons:

- They contain the β -diketonate ligand which generally imparts volatility to metal-organic complexes, particularly when fluorinated, as a result of a reduction in hydrogen-bonding in the solid-state.
- They are capable of systematic substitution through both the β -diketonate and Lewis base ligands to tailor volatility and reactivity.
- Lewis bases such as phosphines, olefins and alkynes are unlikely to thermally decompose at temperatures where copper deposition occurs.
- These precursors can deposit copper via thermally induced disproportionation reactions and no ligand decomposition is required since the volatile Lewis base the Cu(II) disproportionation products are transported out of the reactor intact at the disproportionation temperature.

6.7.4.2 Reaction mechanism

A general feature of the reactions of Cu(I) precursors is that they thermally disproportionate, a mechanism likely to be responsible for the high purity of the copper films observed since ligand decomposition does not occur. The disproportionation mechanism is shown in Figure 6.25 for $(\beta\text{-diketonate})\text{CuL}$. The unique capabilities of this class of compounds result from this reaction mechanism by which they deposit copper. This mechanism is based on the dissociative adsorption of the precursor to form $\text{Cu}(\text{hfac})$ and L, disproportionation to form $\text{Cu}(\text{hfac})_2$ and Cu and desorption of $\text{Cu}(\text{hfac})_2$ and L.

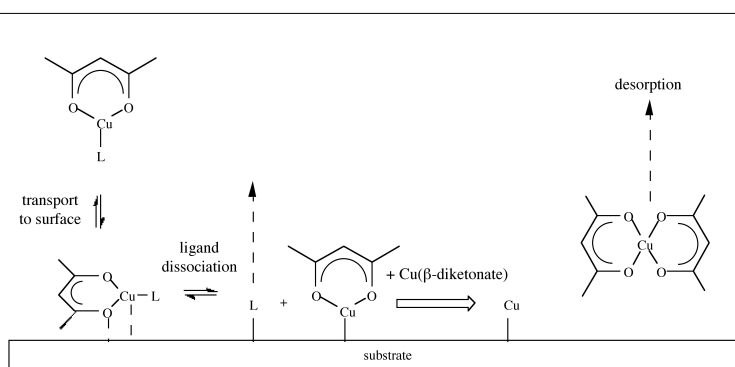


Figure 6.25: Schematic diagram of the disproportionation mechanism. Adapted from T. Kodas and M. Hampden-Smith, *The Chemistry of Metal CVD*, VCH Publishers Inc., New York, NY (1994).

Thus, the starting material acts as its own reducing agent and no external reducing agent such as H_2 is required. Another advantage of the Cu(I) β -diketonates over the Cu(II) β -diketonates is that in the former the ligand L can be varied systematically, allowing the synthesis of a whole series of different but closely related compounds.

6.7.5 Selectivity

Selectivity deposition has been studied in both hot- and cold-wall CVD reactors as a function of the nature of the substrate, the temperature of the substrate and the nature of the copper substituents. Selectivity has

usually been evaluated by using Si substrates on which SiO₂ has been grown and patterned with various metals by either electron-beam deposition, CVD or sputtering. Research has suggested that selectivity on metallic surfaces is attributable to the biomolecular disproportionation reaction involved in precursor decomposition.

6.7.6 Bibliography

- J. R. Creighton, and J. E. Parmeter, *Critical Review in Solid State and Materials Science*, 1993, **18**, 175.
- L. H. Dubois and B. R. Zegarski, *J. Electrochem. Soc.*, 1992, **139**, 3295.
- J. J. Jarvis, R. Pearce, and M. F. Lappert, *J. Chem. Soc., Dalton Trans.*, 1977, 999.
- A. E. Kaloyeros, A. Feng, J. Garhart, K. C. Brooks, S. K. Ghosh, A. N. Sazena, and F. Luehers, *J. Electronic Mater.*, 1990, **19**, 271.
- T. Kodas and M. Hampden-Smith, *The Chemistry of Metal CVD*, VCH Publishers Inc., New York, NY (1994).
- C. F. Powell, J. H. Oxley, and J. M. Blocher Jr., *Vapor Deposition*, John Wiley, New York (1966).
- S. Shingubara, Y. Nakasaki, and H. Kaneko, *Appl. Phys. Lett.*, 1991, **58**, 42.